Post-Earthquake Condition Assessment and Seismic Upgrading Strategies for a Heritage-Protected School in Petrinja, Croatia

Salaman, Aida; Stepinac, Mislav; Matorić, Ivan; Klasić, Mija

buildings

MDPI

Article

Post-Earthquake Condition Assessment and Seismic Upgrading Strategies for a Heritage-Protected School in Petrinja, Croatia

Aida Salaman [1], Mislav Stepinac [2,*], Ivan Matorić [3] and Mija Klasić [3]

[1] Elea iC d.o.o.—Zagreb Branch Office, 10000 Zagreb, Croatia
[2] Faculty of Civil Engineering, University of Zagreb, 10000 Zagreb, Croatia
[3] Peoples Associates Structural Engineers—Zagreb Office, 10000 Zagreb, Croatia
* Correspondence: mislav.stepinac@grad.unizg.hr

Abstract: Following the Zagreb earthquake in March of 2020, a destructive 6.2 magnitude earthquake struck Croatia again in December of 2020. The Sisak-Moslavina county suffered the most severe consequences; many historical and cultural buildings were badly damaged. In the education sector, 109 buildings were damaged. One such building is the case study of this research. The heritage-protected building of the First Primary School in Petrinja is an unreinforced masonry structure, constructed using traditional materials and building techniques. The historical background of the building and the results of the post-earthquake assessment are presented. A numerical calculation of three strengthening methods was performed in 3Muri software: FRCM, FRP, and shotcrete. Non-linear pushover analysis was performed for each model. Finally, the strengthening methods are compared based on the achieved earthquake capacity, cost, and environmental impact.

Keywords: Petrinja; school; earthquake; FRP; FRCM; shotcrete; renovation; assessment; 3Muri; pushover

Citation: Salaman, A.; Stepinac, M.; Matorić, I.; Klasić, M. Post-Earthquake Condition Assessment and Seismic Upgrading Strategies for a Heritage-Protected School in Petrinja, Croatia. *Buildings* **2022**, *12*, 2263. https://doi.org/10.3390/buildings12122263

Academic Editor: Tiago Miguel Ferreira

Received: 14 November 2022
Accepted: 15 December 2022
Published: 19 December 2022

1. Introduction

Recent earthquakes in the Mediterranean once again confirmed the high seismic vulnerability of unreinforced masonry buildings. Thousands of buildings were damaged or demolished by earthquakes in the last 3 years in Albania [1], Greece [2,3], Turkey [4,5], and Croatia [6,7]. The year 2020 in Croatia was marked by two catastrophic earthquakes which caused enormous socioeconomic and material damage in the capital city of Zagreb and surrounding counties. The consequences of the earthquakes are severe: eight fatalities, hundreds of families displaced across the country, and many buildings of great historical and cultural importance damaged or collapsed.

The devastating consequences of the Zagreb earthquake are explained in greater detail in [6,8]; however, the focus of this paper will be on the impact of the 2020 Petrinja earthquake on the historic district of Petrinja, particularly on one typical heritage-protected masonry building. A case study of a heavily damaged primary school in Petrinja is used to showcase the most common types of building damage, as well as seismic strengthening methods for unreinforced masonry buildings.

On 29 December 2020, the Sisak-Moslavina county was struck by a 6.2 M_L earthquake. The maximum intensity of the earthquake in the epicenter was estimated to be VIII–IX on the European Macroseismic Scale [9]. The Petrinja earthquake intensity is shown in Figure 1. The earthquake caused enormous material damage. In Sisak-Moslavina county, where the most affected cities, Petrinja, Glina, and Sisak, are located, the damage is estimated at EUR 4.8 billion and the cost of reconstruction at nearly double—EUR 8.4 billion [10]. According to the data collected by the Croatian Center for Earthquake Engineering (HCPI—in Croatian), more than 57,000 buildings were damaged [11].

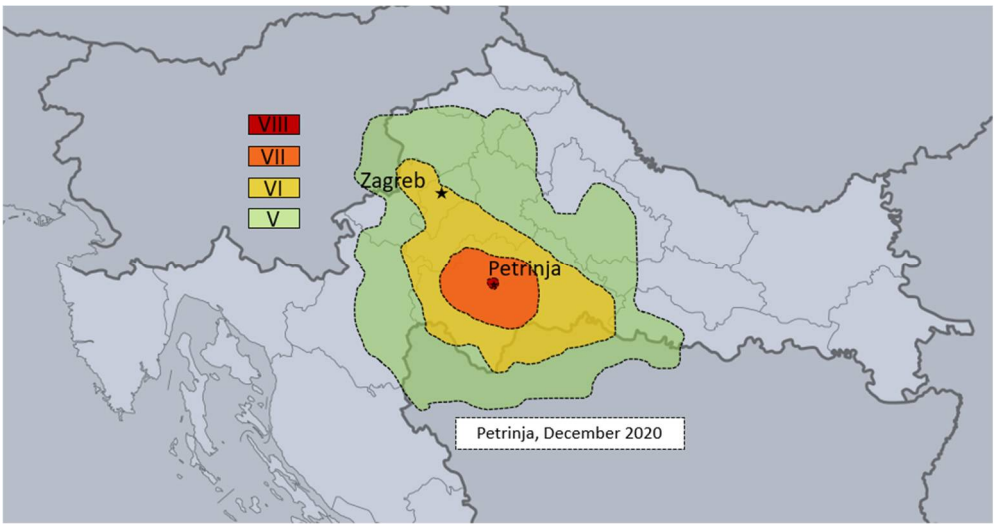

Figure 1. Petrinja earthquake intensity map according to EMS-98.

The Petrinja earthquake was devastating for buildings in the education sector, which suffered the greatest damage in Zagreb and Sisak-Moslavina counties. According to the data from the World Bank report [10] and HCPI [11], as many as 271 buildings were damaged in the earthquake, including 70 kindergartens, 160 primary schools, 32 secondary schools, 3 higher education buildings, and 6 student dormitories in the Sisak-Moslavina, Zagreb, Karlovac, Krapina-Zagorje Counties, and the City of Zagreb. All buildings are public assets, except for six kindergartens in Zagreb County. Most of the buildings were designated as usable or usable with a recommendation. In Sisak-Moslavina County, 109 buildings were damaged. In total, 18 were marked as temporarily unusable and 14 as unusable (1 kindergarten, 9 primary and 4 secondary schools). Some of these buildings require complete reconstruction or should be demolished and rebuilt again. Two photos of damaged buildings after the Petrinja earthquake in the historical center of the city of Petrinja are shown in Figure 2.

Figure 2. Damaged buildings in the historical center of Petrinja.

The total amount of losses and damage in the education sector from the Petrinja earthquake is estimated at EUR 174 million. Out of the total amount, the damage caused to buildings is estimated at EUR 154 million. The remaining EUR 20 million is equal to losses which include the costs of demolition and removal of unusable buildings, protection of cultural heritage buildings, transportation of students to other schools during reconstruction, etc. Over 3000 students were relocated to other schools after the earthquake to continue their education.

Although there were some initiatives for defining seismic risk and vulnerability of buildings in Croatia [12,13], the research was mainly carried out just from a scientific point of view, and the results were not respected by policy makers. Recently, several researchers were dealing with the vulnerabilities of existing educational buildings [14–20] and case studies were presented [21,22]. However, that kind of studies does not exist for Croatian building typologies.

As seismic preparedness was absent, the legislative procedures for the reconstruction were brought very late. The Law on Reconstruction of Earthquake-Damaged Buildings in the City of Zagreb, Krapina-Zagorje County, and Zagreb County [23] was issued six months after the Zagreb earthquake, but it wasn't well prepared and focused solely on the damaged areas in the first earthquake in 2020. As the Petrinja earthquake occurred 3 months after the "well-prepared" Law, modifications to the Law needed to be made. In the end, in February 2021, the new Law on Reconstruction of Earthquake-Damaged Buildings in the City of Zagreb, Krapina-Zagorje County, Zagreb County, Sisak-Moslavina County and Karlovac County was issued [24]. The Law and the Amendment to the Technical Regulation for Building Structures (Official Gazette 75/2020) [25] define four different levels of reconstruction of earthquake-damaged structures in relation to the achieved mechanical resistance and stability. In renovating, every building has to achieve the level of earthquake resistance that is required by HRN EN1998 [26]. The levels of reconstruction according to the Technical Regulation for Building Structures [25] depend on the degree of damage, the importance and purpose of the building, and the financial backing by the investor. The relationship between the selected reconstruction level and the duration/price of the reconstruction is shown in Figure 3. More details about the renovation levels can be found in [7]. It must be said that the rapid post-earthquake assessments and all the following procedures regarding the renovation, developments of legislation, etc. were based on Italian experiences [27–32].

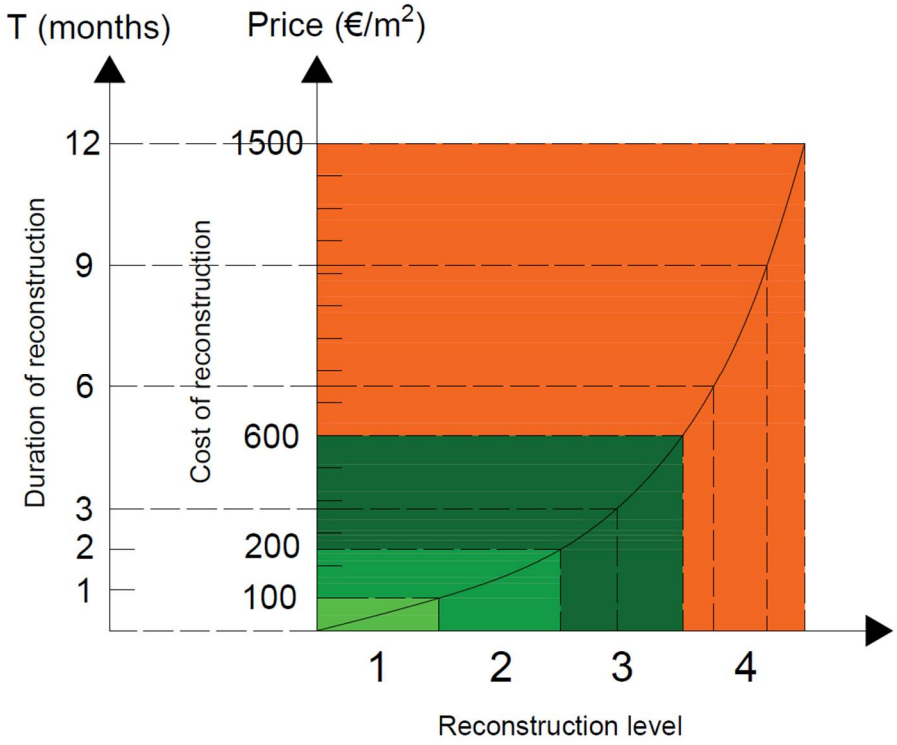

Figure 3. The relationship between the selected reconstruction level and the duration/cost of the reconstruction.

Figure 4 shows the difference between the actual seismic resistance level of the building and the seismic resistance ensured by different levels of reconstruction.

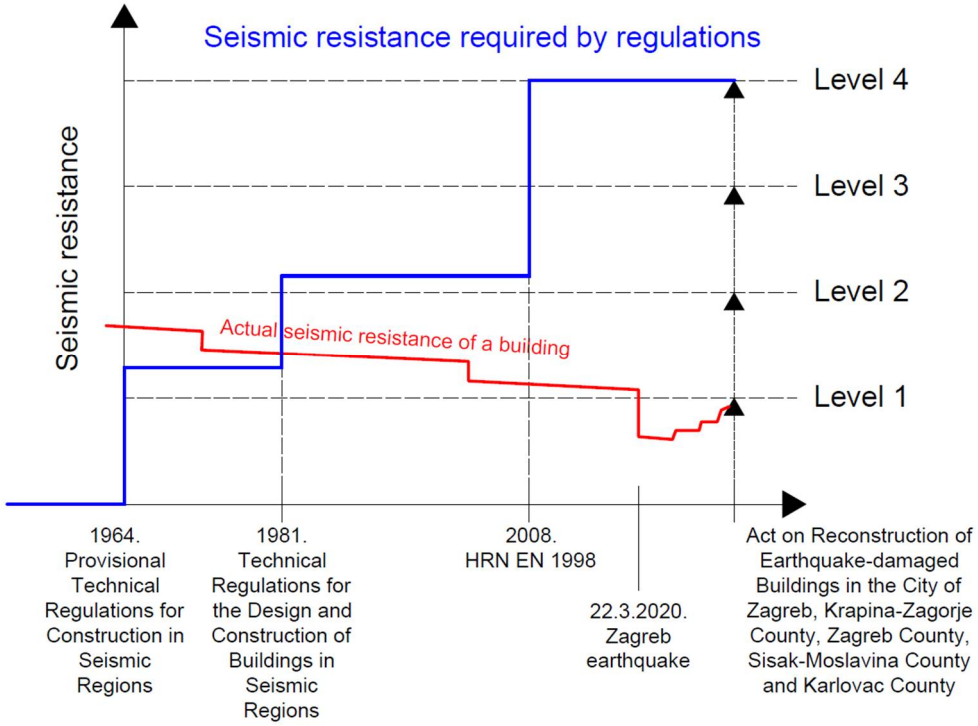

Figure 4. Schematic representation of the reconstruction levels in relation to the actual level of the building's seismic resistance capacity.

In Croatia, unreinforced or partially reinforced masonry buildings make up a large percentage of its building stock. Due to a lack of confining elements, the walls of these buildings almost exclusively transfer compressive loads, while tension causes the appearance of cracks [33,34]. Figure 5 shows some flaws of URM (unreinforced masonry) which cause its poor seismic performance.

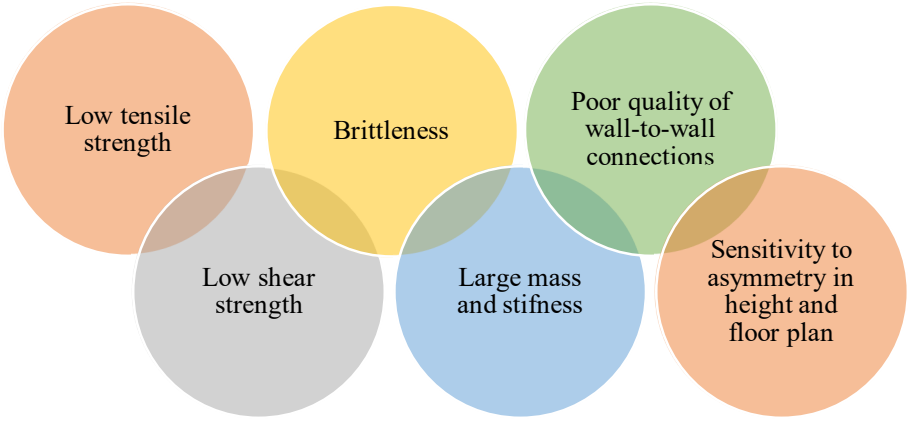

Figure 5. Typical characteristics of unreinforced masonry structures in Croatia.

In Sisak-Moslavina county the most common form of housing is low-rise, usually two-story residential buildings which were built during the post-war reconstruction period in the mid-to-late 1990s. A large percentage of these low-rise residential buildings are URM buildings whose walls were constructed using solid clay bricks and lime mortar of poor quality. The foundations are assumed to be either thin concrete slab or strip foundations. Based on the available, albeit limited, data, it can be assumed the soil is composed of layers of sand, gravel, or thick clay with low bearing capacity and large deformability. The ground floor of these buildings very often lacks vertical confining elements. The facades usually aren't protected by plaster. Horizontal confining elements are either missing or

have insufficient height. The floor structure is usually a thin reinforced-concrete slab or a semi-precast masonry/concrete floor. The roof structures are mainly made of timber. The poor quality of construction and lack of confining elements, which are essential in seismic areas, can be linked to the lower financial status of the residents in the earthquake-affected areas. The most commonly observed types of damage in URM buildings include a partial collapse of gable walls, wall failure due to lack of confining elements, and in-plane shear failure.

In this paper, one heavily damaged school will be presented as a case study. A simple overview of construction practices in Croatia with the historical background of the educational sector in the region is very briefly shown. The assessment procedure and damage classification are explained. However, the focus of this research is to show different strengthening methods for a structural upgrading of a heritage-protected masonry building. A decent number of novel technologies for the seismic upgrading of existing buildings exist on the market. They can be divided as local or global measures as follows:

- Local: FRP (fiber-reinforced polymers)-based systems [35–37], FRCM (fabric-reinforced cementitious matrix)-based systems [38,39], concrete shotcreting [40], reinforcing with steel members and connection retrofitting [41,42];
- Global: capacity increase (new bracing systems, new reinforced shear walls, different additions of shear walls), integrity enhancement (especially for masonry buildings), demand reduction (base isolation, seismic dampers, energy dissipation systems) [43].

Three different, but most common, strengthening strategies are analyzed: strengthening with FRP, FRCM, and concrete shotcrete. The strategies are compared in points of seismic resistance, costs, and very basic environmental impacts.

2. Case Study

2.1. The Founding of the First Primary School in Petrinja—Historical Background

Near the end of the 18th and during the 19th century, the Military Frontier, a military province that the Habsburg Monarchy founded to defend itself against the Ottoman Empire, lost its defensive role and became a burden for the impoverished imperial treasury. The authorities in Vienna attempted to improve conditions by founding new, privileged Frontier cities where the development of crafts and trade was encouraged. These cities/towns soon became economic centers with a large influx of people and goods not only from the surrounding area but also from the more distant parts of the Habsburg Monarchy. It was these immigrants who participated in the work of schools and cultural institutions. The construction practices were similar to those in other major cities in the Monarchy [6,13,44,45]: URM buildings (brick masonry of format 29 × 14 × 7 cm) with timber floors and roofs.

The educational reform of Maria Theresa in 1764, which ordered that a German school must be founded in all important cities of the Military Frontier, was extremely important for this area. The main task of these schools was to train a certain number of literate people for the Frontier army. Up until then, schools were founded by nobles and church orders, and the church authorities oversaw the schools.

As a result of these reforms, the public school in Petrinja became a Normal School (*dt. Normalschule*) in 1777. The building of the Normal School was built in 1780. In 1861 the old, dilapidated timber building was demolished, and a new single-story masonry building was built in its place. The plans for the building were made by Croatian architect Bonifacio Cettola. The construction of the building was completed in 1862, and the new building (which today houses the First Primary School) was said to be the most beautiful school in the Military Frontier. In 1871, the construction of a neighboring two-story neo-Renaissance building was completed, which today houses the Petrinja High School (Figure 6).

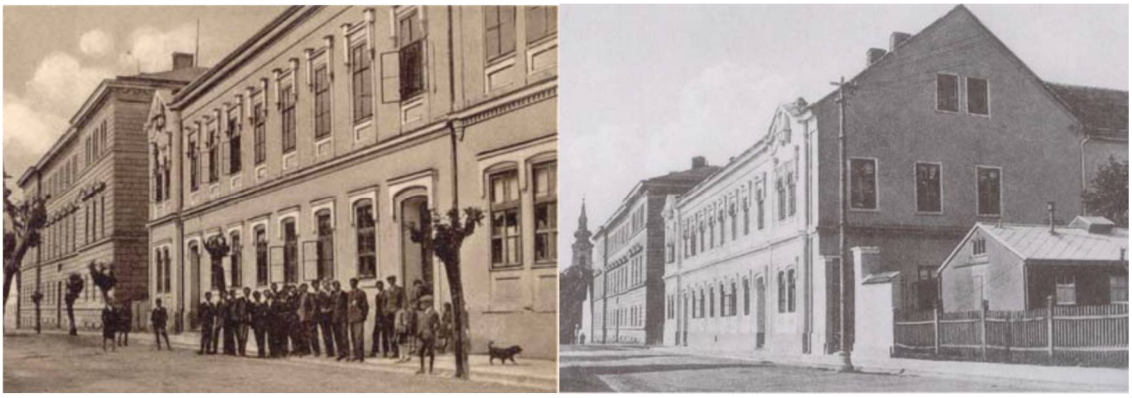

Figure 6. The building of the First Primary School in Petrinja in the 1930s [46].

During the Croatian War of Independence (1991–1995), the school was used as a warehouse for clothes and food. After the liberation of Petrinja in 1995, the building was in poor condition due to aging and lack of maintenance. It had also been damaged during the war. Renovation works lasted until June 1996, when students began to attend classes again. More than a decade later, in June 2007, a much-needed reconstruction of the building structure was carried out since the previous works were mainly for aesthetic purposes. The building was restored to its former glory and classes continued regularly until the devastating Petrinja earthquake in December 2020, when the building suffered considerable damage.

Today the building of the First Primary School is located in the cultural district of the city of Petrinja and, due to its long history and tradition, is classified as a cultural heritage building. The building is listed in the Register of Cultural Properties of the Republic of Croatia and is protected by the Act on the Protection and Preservation of Cultural Goods.

2.2. Description of the Case Study

The building of the First Primary School consists of two units: the main building and the auxiliary building, which is detached from the main building. In the second half of the 20th century, a vestibule was built between the courtyard wings as a single-story, reinforced concrete structure, with a second floor added in 2007. The main building has a U-shaped floor plan; the external dimensions are 36.45 m × 31.10 m. The dimensions of the auxiliary building are 33.39 m × 6.30 m. The dimensions of the courtyard wings are 13.30 m × 16.60 m. The total height of the main building from the ground level is approx. 15.50 m. The height of the auxiliary building is approx. 4.00 m above ground level. The height of the flat roof of the vestibule between the courtyard wings is 8.42 m above ground level. The main building was built in 1862 as an unreinforced masonry structure, and the auxiliary building was built in 2017 as a reinforced concrete structure. The auxiliary building was built in accordance with current regulations; it is detached from the main building and was not damaged in the 2020 Petrinja earthquake. Therefore, it is not the subject of this paper.

The main building achieved its current floor plan (Figure 7) in the second half of the 20th century when the wings on the eastern side were upgraded, and their length increased by 7 m. Various adaptations, upgrades, and reconstructions of parts of the building have been carried out over the years.

On the ground floor the ceiling structure is a masonry barrel vault, reinforced with steel beams. The floor structure in the sanitary areas in both upgraded wings, as well as the vestibule, is a concrete slab. In the classrooms on the first floor, the floor structure is timber—the floor joists are 90 cm apart. Walls are constructed using solid brick elements 30 × 15 × 7 cm and lime mortar. The total thickness of the walls varies from 50 to 100 cm, including layers of plaster. The thickness of the outer load-bearing walls varies from 81 to 96 cm, and of the inner load-bearing walls from 51 to 67 cm. The staircases are U-shaped

and made of timber. The load-bearing roof structure is timber. The original plans of the foundations, and the structural analysis and design of the building are not available. The structure of the vestibule is constructed using reinforced concrete columns and beams with a semi-precast masonry/concrete ceiling. Figure 8 shows the 3D models of the floors of the main building without the added vestibule, which are modeled and calculated in this paper. Grey parts represent secondary walls without a load-bearing function.

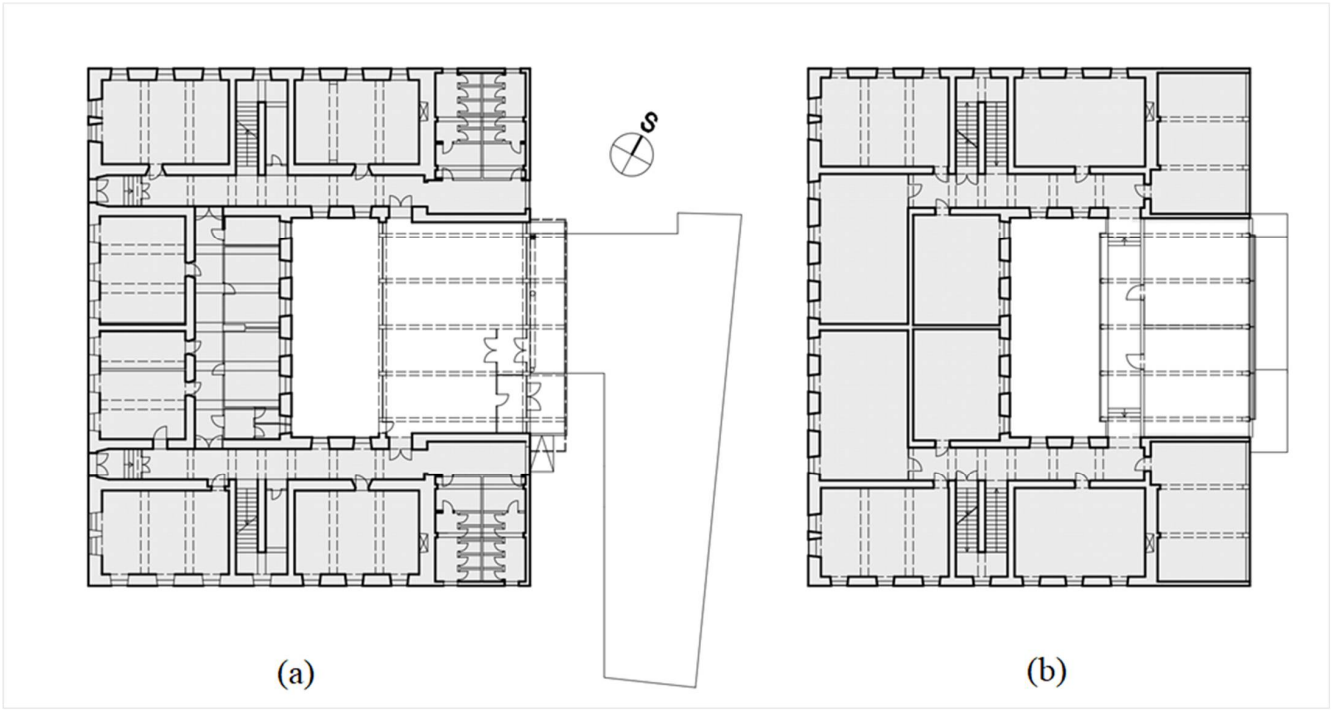

Figure 7. Floor plans: (**a**) ground floor; (**b**) first floor.

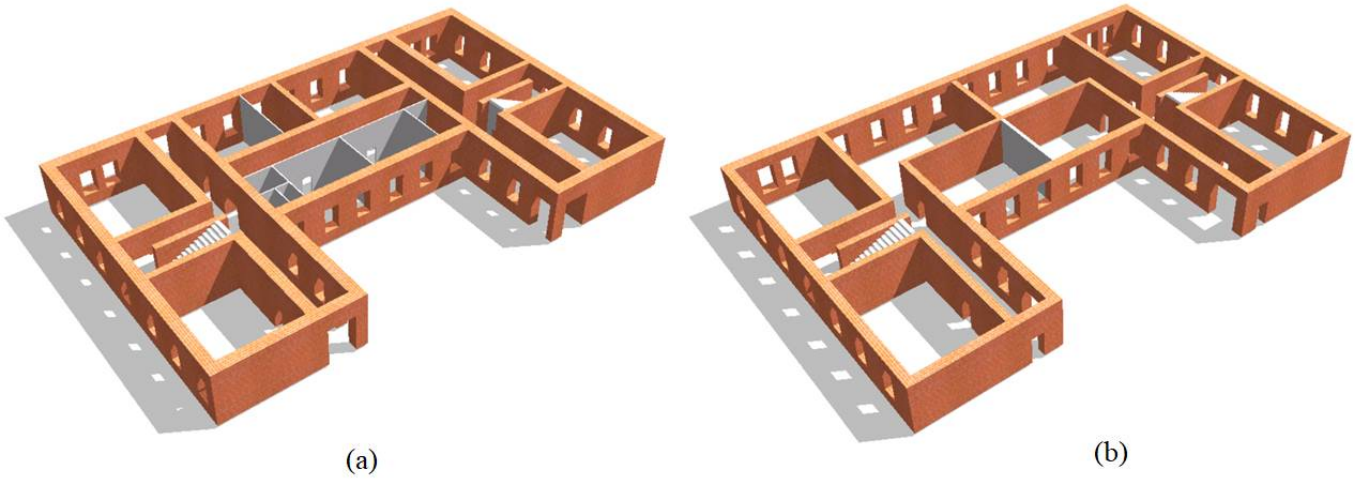

Figure 8. 3D models of: (**a**) the ground floor; (**b**) the first floor.

2.3. Post-Earthquake Damage Assessment

Following the rapid post-earthquake assessment, the building was assigned the N2 label—not usable due to damage, which means that the structure has reached its load-bearing capacity, and there is a possibility of a collapse of load-bearing and non-load-bearing elements. For a full description of the post-earthquake procedures and damage grading the reader is addressed to [47–50].

A more detailed inspection was carried out in April 2022 within the detailed condition assessment. The following damage was recorded: on the north-western side of the building the roof structure had collapsed, which also caused part of the timber floor structure below it to collapse; the north-western and south-eastern gable walls have collapsed; horizontal cracks are visible on the western gable walls, indicating out-of-plane damage (Figures 9–12). Furthermore, the masonry arches in the vicinity of the staircase on the ground floor were damaged, and part of the barrel vault on the first floor had collapsed. The collapsed vault is near the area of the building where the roof and timber floor structure had collapsed. More detailed failures are explained in Table 1.

Figure 9. Southwestern façade plan with marked damage.

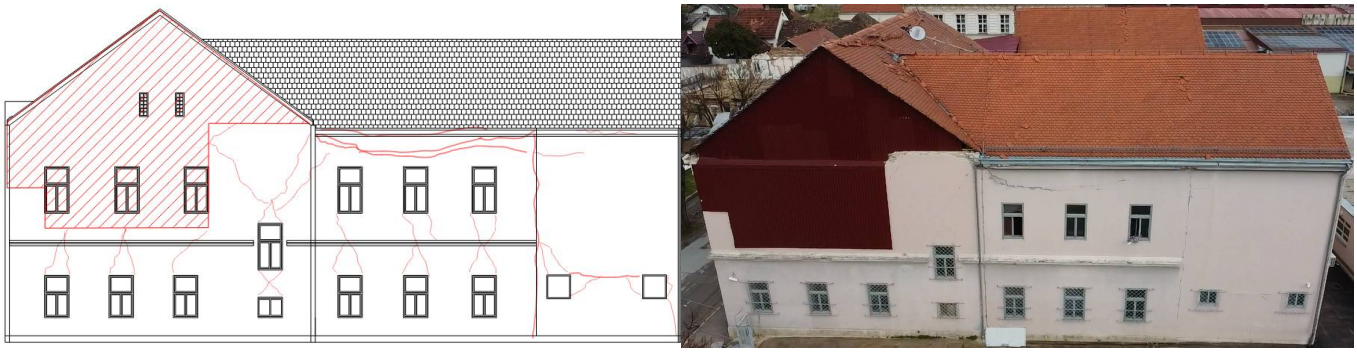

Figure 10. Southeastern façade plan with marked damage.

Figure 11. Northwestern façade plan with marked damage.

Figure 12. Northeastern façade plan with marked damage.

Considering the findings of the detailed inspection, the damage to the building is classified as Grade 4: very heavy damage (heavy structural damage, heavy non-structural damage), according to the EMS-98 classification [9] of damage.

Table 1. Typical damages of the case-study building.

Recorded Building Damage	
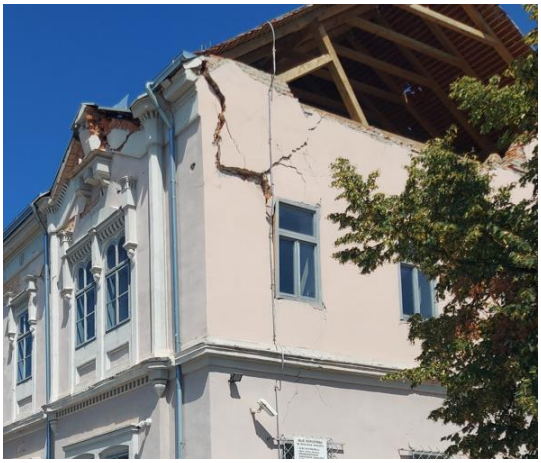	
Out-of-plane failure of wall connections	Partial overturning of the gable walls
	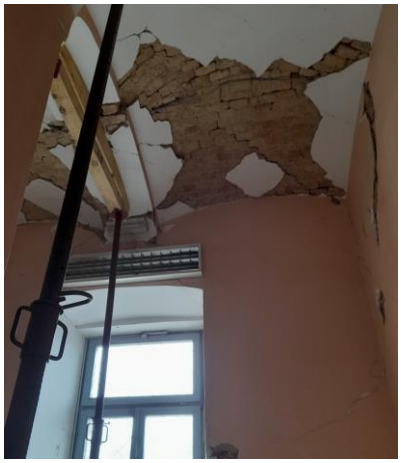
Out-of-plane wall failure in the attic	Vault damage/collapse

Table 1. *Cont.*

Recorded Building Damage	
	
In-plane shear failure of interior walls	In-plane sliding failure (horizontal cracks)
	
In-plane shear failure (diagonal cracks)	Tensile failure of masonry and vertical cracks at the corners
	
Shear failure of spandrels (diagonal cracks)	Partial collapse of the floor structure

In addition to the detailed inspection of the building, basic investigative works were also carried out to determine the material properties. Floor structures were examined to determine the type and thickness of layers and structural timber elements; the wall thickness and the dimensions of the brick elements were measured; mechanical properties of masonry walls (compressive strength and shear strength) were measured at two locations.

One of the hardest things about this building was to decide the exact locations of in-situ testing. Half of the building's roof collapsed and was under influence of external environmental conditions such as wind, rain, and snow. In addition, the facade walls are full of openings, so they were not suitable for testing. The chosen wall should be undisturbed, load bearing, if it is possible without openings, without any damage, etc.

The selected load-bearing walls are not in the vicinity of the collapsed parts of the building; they were not exposed to the weather or damaged, and have as few openings as possible. The compressive strength was tested in the field by directly loading the brick in the wall with a cylindrical press, and brick samples were taken from the building in six different places so that they could be tested in the laboratory for uniaxial compressive strength. Shear strength was measured "in situ" by using a hydraulic press. The mortar was moved horizontally in the vicinity of one brick in order to determine the shear strength. At the same time, the structure of the existing wall was minimally damaged. One brick is isolated in the wall so that it can move on one side, and a hydraulic press is placed on the other side, which applies pressure to the brick until it fails. More explanation of this common procedure in Croatia is given by Lulić et al. [49].

The following values were obtained after in situ testing:

- Shear strength of masonry under zero normal stress, f_{v0} = 0.05–0.06 N/mm^2;
- Compressive strength of the brick elements, f_b = 7.00 N/mm^2.

3. Modelling and Design of Seismic Strengthening Methods

Although, the research on complex and more precise modeling of URM is very active [51–54], in this research the 3D model for the evaluation of the seismic behavior was created in the 3Muri software [55], which is used for the analysis of new or existing buildings, and is especially suitable for performing non-linear static (pushover) analysis, which provides very good results for masonry structures.

Furthermore, the 3Muri software can perform linear static analysis and modal analysis according to Eurocode 6 [56] and Eurocode 8 [26]. The 3Muri uses the FEM—Frame by Macro Element calculation method [57,58]. Once the 3D model of the building is created, the generation of the equivalent frame model transforms every wall element into several deformable pier and spandrel elements, which are connected by rigid nodes. Provisions given by Italian researchers [59,60] about the modeling and seismic response analyses of URM buildings were respected.

Modeling in 3Muri software can be divided up into four phases:

- Phase 1: definition of geometry;
- Phase 2: definition of structural characteristics;
- Phase 3: model analysis;
- Phase 4: structural analysis;
- Optional phase 5: local mesh.

Every object is characterized by its material and geometric properties. Definition of structural characteristics consists of defining material, geometrical, and structural properties. Material properties can be obtained through investigation work, assumed based on Eurocode, MQI method, NDTs, etc. Geometrical properties are obtained through research of archive and existing documentation, site visiting, and assessment. Structural analysis is performed after all structural objects have been defined.

Structural analysis of the model consists of gravity (static) analysis, bending analysis out of plane, linear analysis, modal analysis, and non-linear analysis (pushover analysis). Results of performing non-linear analysis consist of capacity curves, vulnerability indices, damage to the building, periods, activated masses, etc.

The program automatically generates constraints and boundary conditions of the elements; however, additional constraints can be manually defined. For existing structures which have suffered damage during an earthquake (as is the case with First Primary School in Petrinja), one way of verifying the effectiveness of the model is a comparison of actual,

recorded damage with the results of the pushover analysis. The result of the pushover analysis is the capacity curve. The deformation of every wall can be shown in every step of the analysis with color-coded damage (for example, red color is bending damage, orange is shear damage). If the building model is accurate, the recorded damage will, in certain measure, correspond with the results of the pushover analysis for any given wall.

The self-weight of the barrel vaults and the timber floors was determined according to the results of the investigation works. The imposed load on the floor structures was determined according to HRN EN 1991-1-1:2012/NA (Category C—areas where people may congregate—areas in schools [61]). The snow load on the roof structure was calculated according to HRN EN 1991-1-3/NA.

For the given location of the building, the ground type C (deep deposits of dense or medium-dense sand, gravel of stiff clay with thickness from several tens to many hundreds of meters) was selected. Considering that the case study has great cultural and historical importance, and is currently being used as a primary school, it is classified as Importance class III, with the corresponding importance factor $\gamma_I = 1.2$. The seismic hazard map for Croatia from the National Annex to Eurocode 8 [62] was used to determine the value of peak ground acceleration (PGA). The design ground acceleration is equal to peak ground acceleration times the importance factor:

For the return period of 95 years:

$$a_{g,95} = \gamma_I \times a_{gR} = 1.2 \times 0.074g = 0.87\ m/s^2$$

For the return period of 475 years:

$$a_{g,475} = \gamma_I \times a_{gR} = 1.2 \times 0.152g = 1.80\ m/s^2$$

Given that the building in question is classified as Importance class III, and that the building was heavily damaged, the chosen reconstruction level for the building is level 4: complete reconstruction of the building structure. At reconstruction level 4, the building's seismic resistance should match the conditions given by the Technical Regulations for Building Structures and HRN EN. The value of the vulnerability index for each of the two limit states (Significant Damage and Damage Limitation) must be greater than 1.00. The vulnerability index α is defined as the ratio between the limit capacity acceleration of the building and the reference peak ground acceleration. For Limit State of Significant Damage, the return period of PGA is 475 years, corresponding to the probability of exceedance of 10% in 50 years. For Limit State of Damage Limitation, the return period of PGA is 95 years, corresponding to the probability of exceedance of 10% in 10 years.

The masonry properties used are based on investigative post-earthquake assessments on similar buildings [48,49,63,64] and are shown in Table 2.

Table 2. Masonry properties.

Material	MoE, [N/mm^2]	Shear Modulus G, [N/mm^2]	Specific Weight [kN/m^3]	Characteristic Compression Strength, [N/mm^2]	Shear Strength [N/mm^2]
Masonry	1500.00	500.00	18.00	1.62	0.05

Linear static analysis of the structure was carried out, and it was concluded that all walls meet the load-bearing conditions and the geometric conditions. Furthermore, a modal analysis was carried out; the results are presented in Table 3.

Another important parameter that needs to be defined for pushover analysis is the control node, whose displacement is used to draw the capacity curve. The control node is located on the top floor and as close as possible to the center of mass. The selected node is shown in Figure 13.

Table 3. Modal analysis results.

Mode	T [s]	m_x [kg]	M_x [%]	m_y [kg]	M_y [%]	m_z [kg]	M_z [%]
1	0.29594	1,829,485	70.37	160	0.01	25	0
4	0.21744	108,720	0.42	2,090,799	80.42	1	0

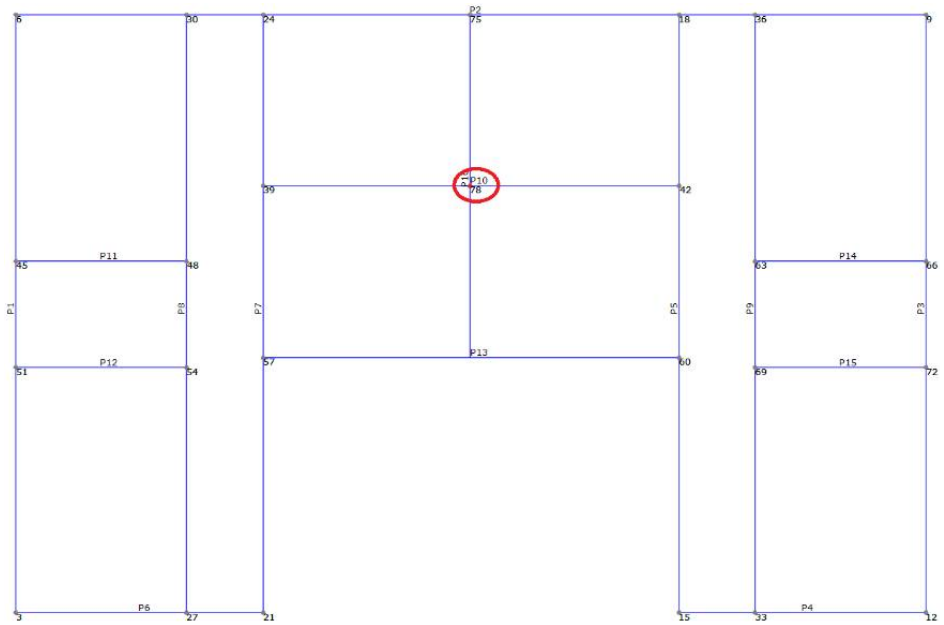

Figure 13. Position of the selected control mode on the top floor.

Local mechanisms were also checked. 3Muri has an optional module that performs local mechanisms analysis. The local mechanisms analysis is performed on those parts of the building where there is a possibility of wall failure by overturning due to an earthquake. To check the local mechanisms, it is necessary to extract from the global numerical model a part of the structure that is assumed to have failed due to overturning; these are usually gable walls or protruding parts of structures. The capacity check is carried out using the kinematic model balance method by comparing the required acceleration that causes the out-of-plane failure of the isolated part of the structure and the minimum required acceleration that depends on the height position of the isolated part of the structure. For the case-study building, gable walls were of course critical.

3.1. Results of the Pushover Analysis

For the case-study building, 24 pushover analyses were performed, depending on the type of load (uniform and modal distribution), direction (±x, ±y) and the accidental eccentricity value which accounts for inaccuracies in the distribution of masses in the structure. As traditional buildings in Croatia, as well as in all the Mediterranean region, consist of load-bearing masonry walls and timber diaphragms, these diaphragms can be considered flexible or semi-flexible. Lately, a lot of research has been done in the field [65–71].

The results of the performed analyses are presented as 24 corresponding capacity curves (Figure 14).

Figure 15 shows a 3D representation of different types of damage to the building at the last step of the pushover analysis. In *x* direction, most of the damage is bending (pink color) and shear (beige and orange color) damage, but serious failure has not yet occurred. This is not the case for the *y* direction where the wall elements of the southwestern façade are in serious crisis (pink color) and are failing during the elastic phase (blue color). This is in accordance with the actual recorded damage of the building.

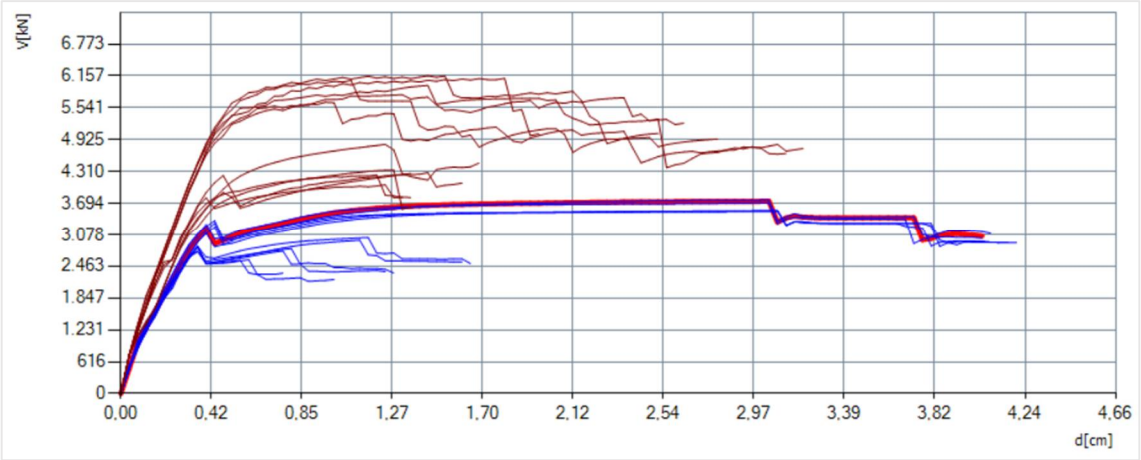

Figure 14. Capacity curves for x (blue) and y (red) direction. The bright red color represents a critical result.

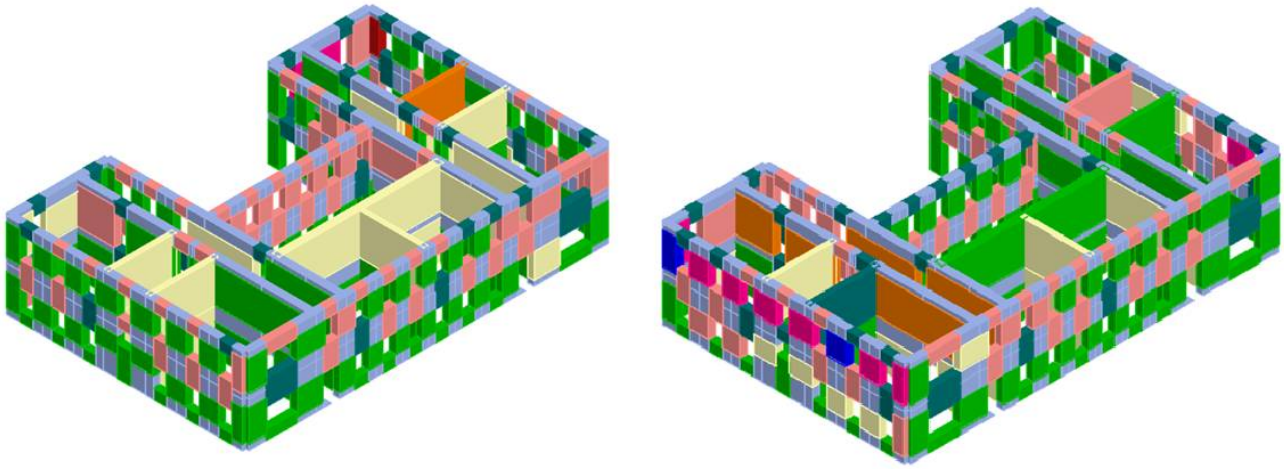

Figure 15. 3D view of damage for the most significant pushover analysis: (**a**) in x-direction; (**b**) in y-direction.

Table 4 shows the values of the vulnerability index for the most significant analysis in the x and y directions. Since the values for both Significant Damage and Damage Limitation limit states are lower than 1.00, it can be concluded that the current building structure is deficient and requires seismic strengthening.

Table 4. Values of vulnerability index α for the most significant analysis in the x and y direction.

No.	Direction	α_{SD}	α_{DL}
12	+X	0.333	0.434
19	+Y	0.569	0.697

Figures 16 and 17 show the comparison of obtained failures by 3Muri and observed damage on the real case-study building.

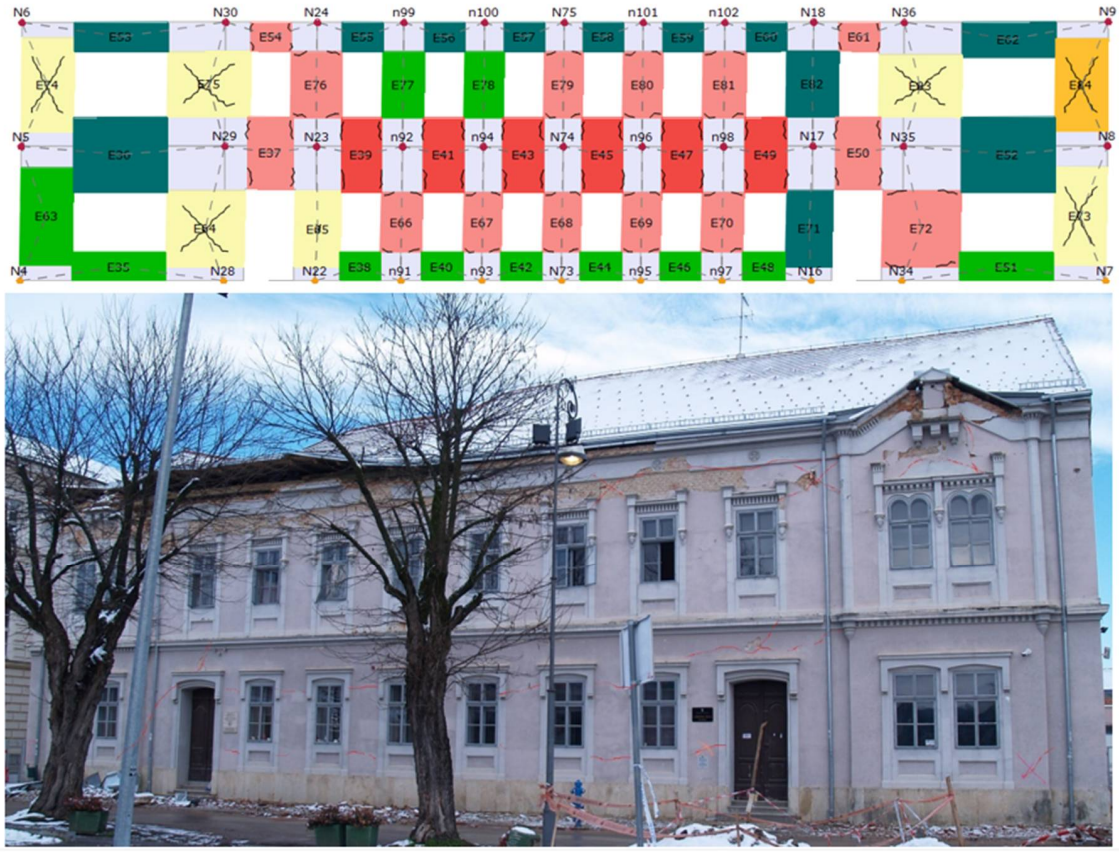

Figure 16. Detailed display of street facade damage in the 3Muri software package and actual damage to the street facade of the building in question.

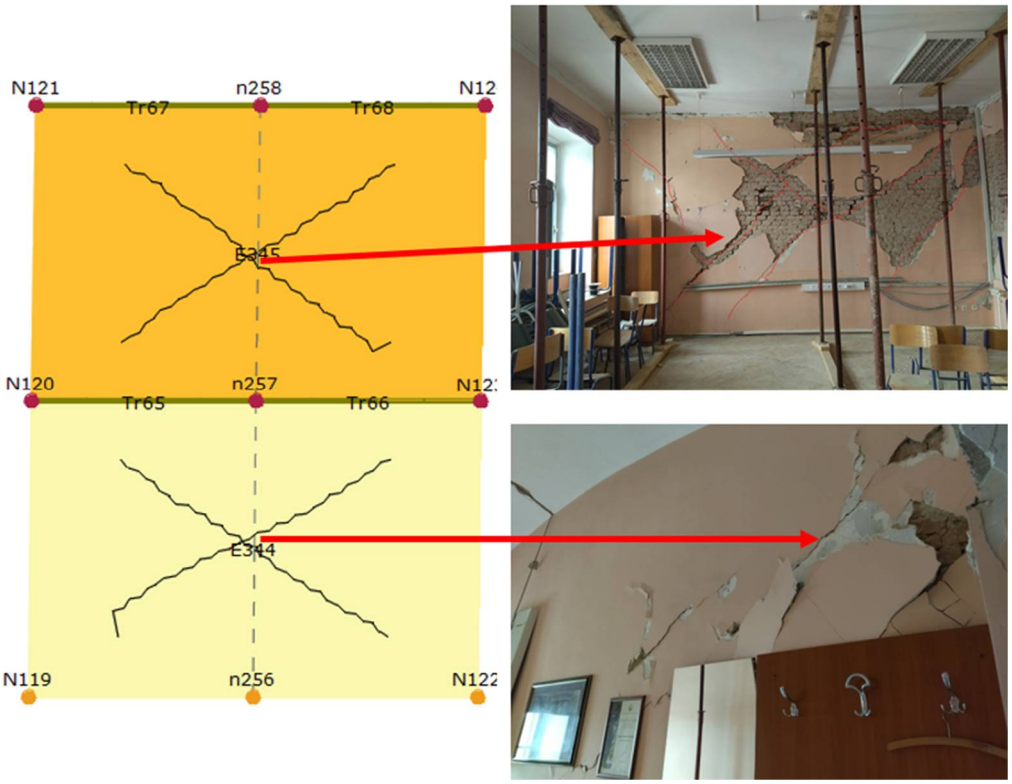

Figure 17. Detailed display of damage in the 3Muri software package and actual damage to the walls of the building in question.

3.2. Seismic Strengthening Strategies

In this paper, the three most commonly applied methods of seismic strengthening in Croatia are presented: reinforcement with concrete shotcrete, with FRP, and with FRCM.

In 3Muri software in the definition of structural characteristics there is a possibility to define retrofitting measurements such as FRCM/FRP, shotcrete, reinforced plaster, reinforced masonry, reinforcement, etc. For FRCM/FRP reinforcement, there is a material library with all the needed data for different providers such as MAPEI, Kerakoll, Ruregold, etc. To apply FRCM or FRP reinforcement, one needs to define which reinforcement and which manufacturer he/she uses. After defining the type of reinforcement and manufacturer, the basic material characteristic should be defined. After that, the software automatically calculates changes in structural characteristics. Applying shotcrete consists of applying reinforcement on masonry walls such as reinforcing mesh and changing the wall MoE so that software can calculate changes in structural characteristics. Before deciding what kind of retrofitting method is the most suited to stabilize the current structure of the building and make the building earthquake-resistant, it is needed to think about how it will affect the building. For example, would it increase the masses of the building, would it modify the structural system, etc. After applying retrofitting measurements, it is necessary to perform model analysis and structural analysis to see if the building has reached the required safety level.

The numerical calculation of all reinforcements was performed for a model with a rigid diaphragm on the first floor (timber–concrete composite floor) because without such a solution it was not possible to meet the limit states of significant damage and limited damage. Although the retrofitting technique for activating timber floors for their energy dissipation is ongoing research [72], still, according to Croatian regulations timber–concrete composite was chosen.

3.2.1. Reinforcement with FRCM

FRCM is a modern and compatible strengthening strategy for existing masonry, which consists in plastering the walls by means of mortar layers with embedded grids or textiles made of long fibers [73]. In this research, the structure is reinforced with five different FRCM systems of varying thicknesses, which are shown in Table 5. Three layers of glass fiber mesh were applied to both faces of the walls to ensure there is no difference in wall stiffness. Glass fiber mesh was chosen due to its availability and cost-effectiveness [74]. The most favorable configuration of different FRCM systems that satisfied the Significant Damage and Limited Damage limit states (Figure 18) was determined by iteration. The results of the pushover analyses are presented as 24 capacity curves (Figure 19).

Table 5. FRCM composite system properties.

FRCM Composite System					
Fiber thickness t_f (mm)	0.18	0.22	0.25	0.28	0.30
Modulus of elasticity E (N/mm^2)			71,000		

3.2.2. Reinforcement with FRP

The structure is reinforced with four different FRP systems of varying thicknesses, which are shown in Table 6. Carbon fiber fabric is applied to both faces of the walls. The most favorable configuration of different FRP systems that satisfied the Significant Damage and Limited Damage limit states (Figure 20) was determined by iteration. The results of the pushover analyses are presented as 24 capacity curves (Figure 21).

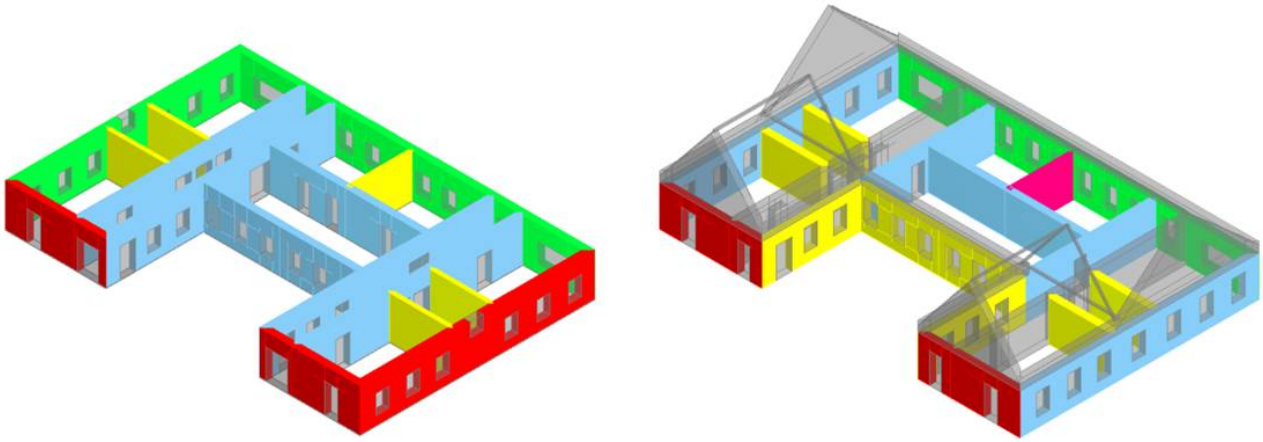

(a) (b)

Figure 18. Configuration of different FRCM systems: (**a**) on the ground floor; (**b**) on the first floor.

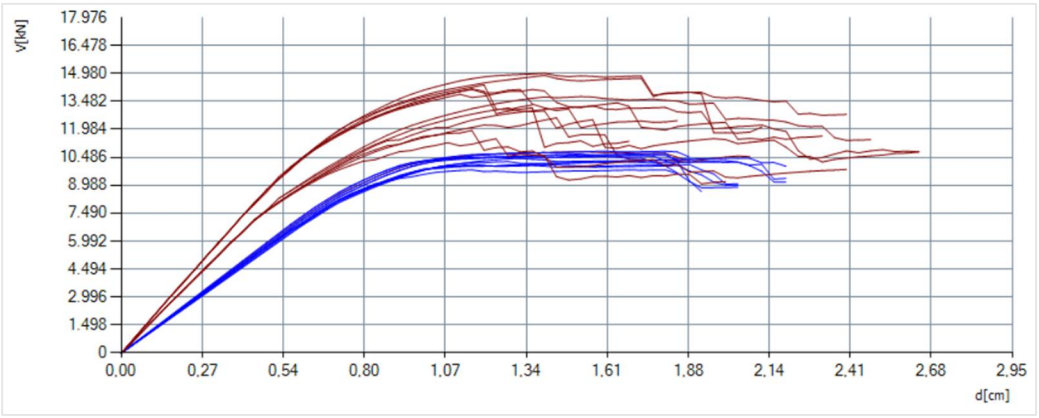

Figure 19. Capacity curves for the model strengthened by FRCM composite system for *x* (blue) and *y* (red) direction.

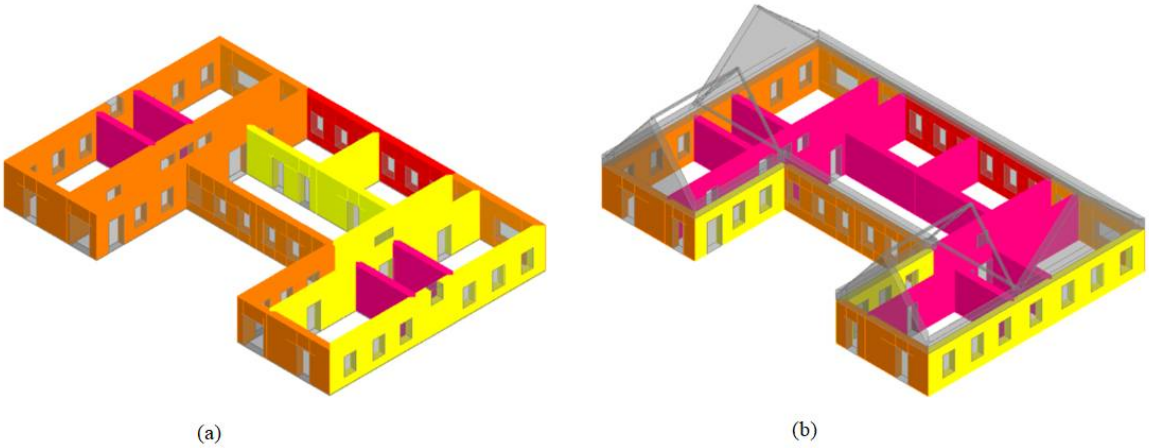

(a) (b)

Figure 20. Configuration of different FRP systems: (**a**) on the ground floor; (**b**) on the first floor.

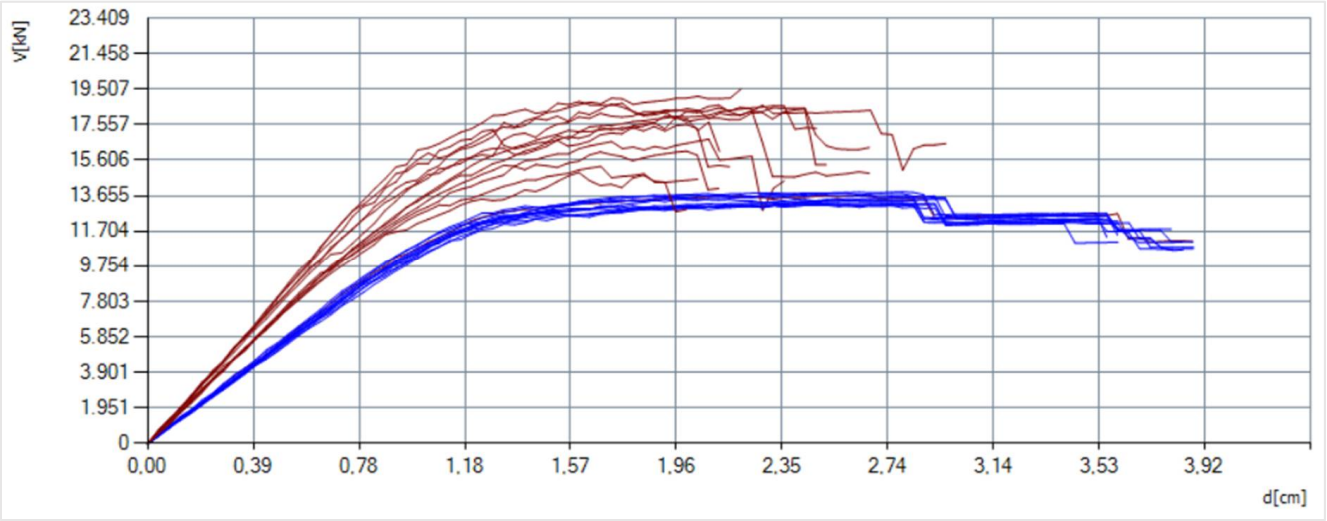

Figure 21. Capacity curves for the model strengthened by FRP composite system for x (blue) and y (red) direction.

Table 6. FRP composite system properties.

FRP Composite System				
Fiber thickness t_f (mm)	0.15	0.18	0.22	0.25
Modulus of elasticity E (N/mm^2)	390,000			

3.2.3. Reinforcement with Concrete Shotcrete

The third and final analyzed method is reinforcement with shotcrete. The thickness of the concrete layer is 6 cm, the selected reinforcing mesh is Q283 (6 mm diameter bars with 100 mm pitch), and the steel grade is B500B. Unlike the previous two strengthening methods, shotcrete is applied to only one face of the wall, given that such a variant meets the required checks, and results in a lower cost of reconstruction. On the external walls, shotcrete is applied on the inner face of the wall to preserve the appearance of the building, which has great cultural and historic importance. The most favorable configuration of shotcrete reinforcement that satisfied the Significant Damage and Limited Damage limit states (Figure 22) was determined by iteration. The results of the pushover analyses are presented as 24 capacity curves (Figure 23).

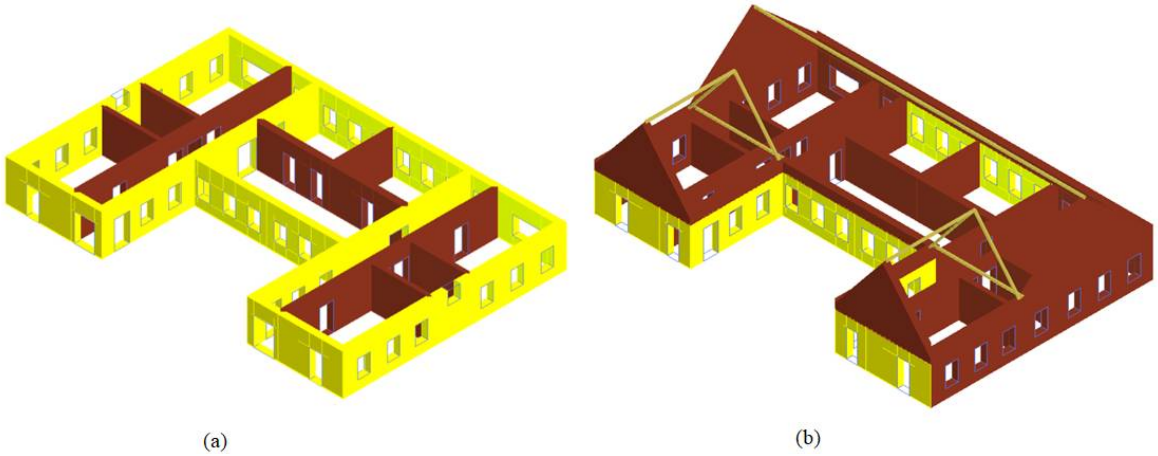

Figure 22. Configuration of shotcrete reinforcement (yellow color): (**a**) on the ground floor; (**b**) on the first floor.

3.3. Comparison of Strengthening Methods

The risk indices of the most significant pushover analysis for both Significant Damage and Damage Limitation limit state are presented in Table 7. The limit state is considered satisfied if the vulnerability index α is greater than 1.00. The vulnerability index α is the result of the pushover analysis and is defined as the ratio between the limit capacity acceleration of the building and the reference peak ground acceleration. Two vulnerability indices are calculated for every pushover analysis: one for Significant Damage LS and one for Damage Limitation LS. The limit capacity acceleration of the building is the peak ground acceleration for which the structure reaches one of the two limit states. For Limit State of Significant Damage, the return period of PGA is 475 years, corresponding to the probability of exceedance of 10% in 50 years. For Limit State of Damage Limitation, the return period of PGA is 95 years, corresponding to the probability of exceedance of 10% in 10 years. The PGA values are input data for seismic load. The value of the vulnerability index for each of the two limit states must be greater than 1.00. The EN 1998-3 defines the Significant Damage Limit State as follows: the structure is significantly damaged, with some residual lateral strength and stiffness, and vertical elements can sustain vertical loads. Non-structural components are damaged, although partitions and infills have not failed out-of-plane. The structure can sustain after-shocks of moderate intensity. The Damage Limitation Limit State can be defined as follows: the structure is only lightly damaged, with structural elements prevented from significant yielding, and retaining their strength and stiffness properties. Non-structural components, such as partitions and infills, may show cracking, but the damage could be economically repaired. EN1998-3 defines a third limit state: Near Collapse; however, the Croatian National Annex doesn't require checks for that LS. Accidental eccentricity of the center of mass with respect to the rigidity center is computed automatically. According to EN1998, it is calculated as 5% of the floor dimension perpendicular to the direction of the seismic action.

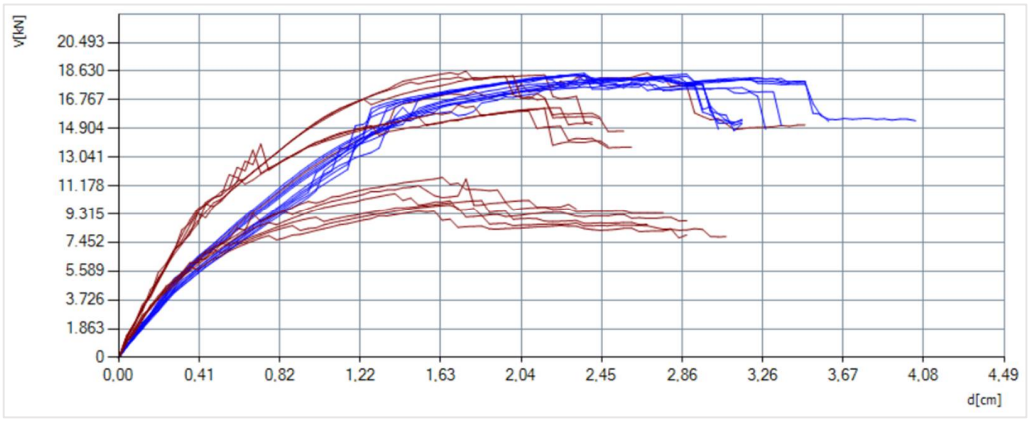

Figure 23. Capacity curves for the model strengthened by shotcrete for the *x* (blue) and *y* (red) direction.

Table 7. Vulnerability indices for the most significant analysis in the *x* and *y* direction for the strengthened models.

Method	No.	Direction	α_{SD}	α_{DL}
FRCM	13	−X	1.002	1.614
FRCM	22	−Y	1.175	2.133
FRP	15	−X	1.522	1.944
FRP	20	+Y	1.257	2.182
Shotcrete	12	+X	1.752	2.861
Shotcrete	19	+Y	1.377	1.912

All 24 pushover analyses for all strengthening methods satisfied this check. A 3D visualization of damage for the most significant analysis in x and y directions for all strengthening methods is shown in Figure 24.

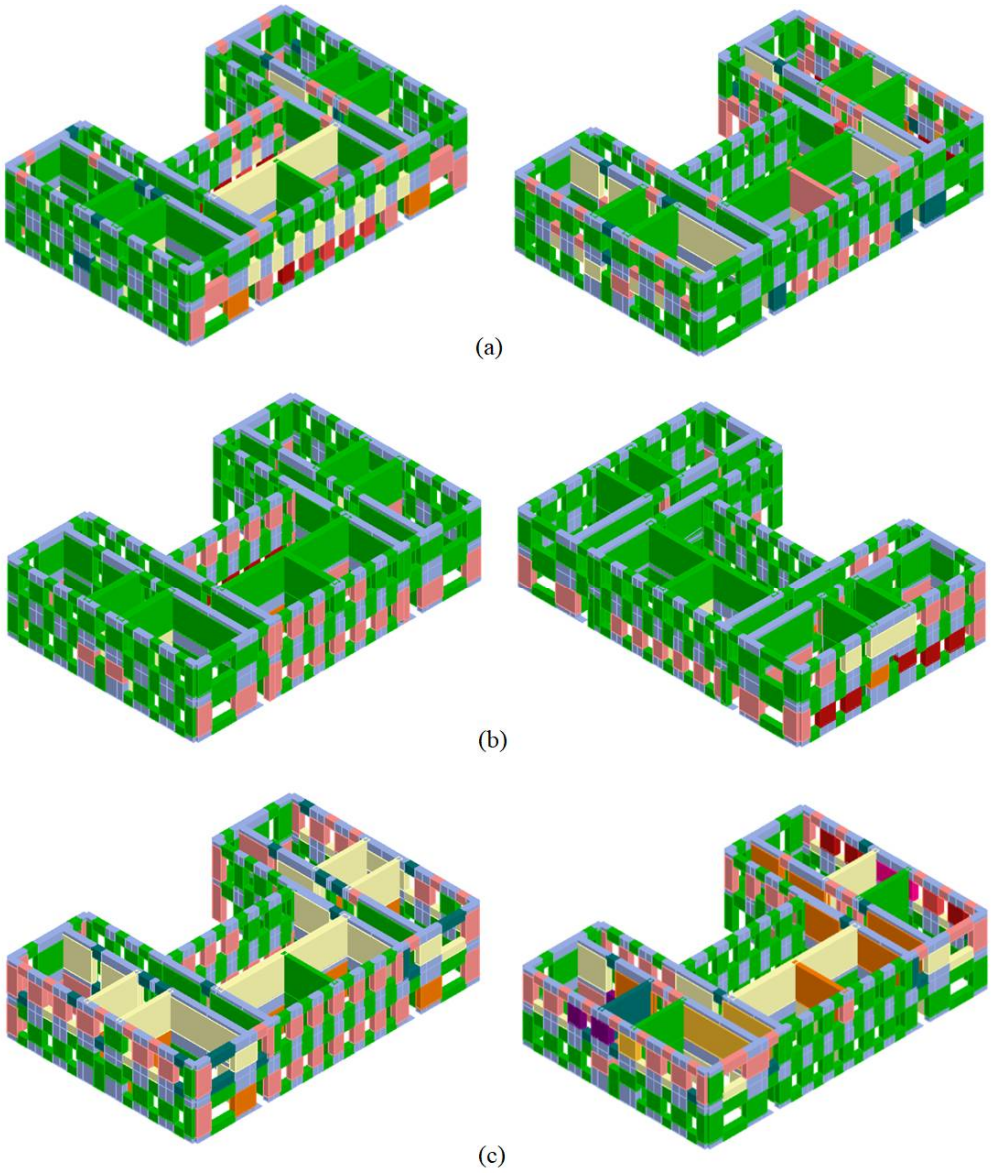

Figure 24. Three-dimensional visualization of damage in the last step of the most significant pushover analyses in *x* and *y* direction: (**a**) FRCM strengthening; (**b**) FRP strengthening; (**c**) shotcrete strengthening.

A graphical comparison of vulnerability indices for all 24 pushover analyses is shown in Figure 25. Figure 26 shows the comparison of the risk indices for the unreinforced model and all reinforcement variants. The results show that the highest values of the vulnerability index are mostly obtained for the model reinforced with shotcrete.

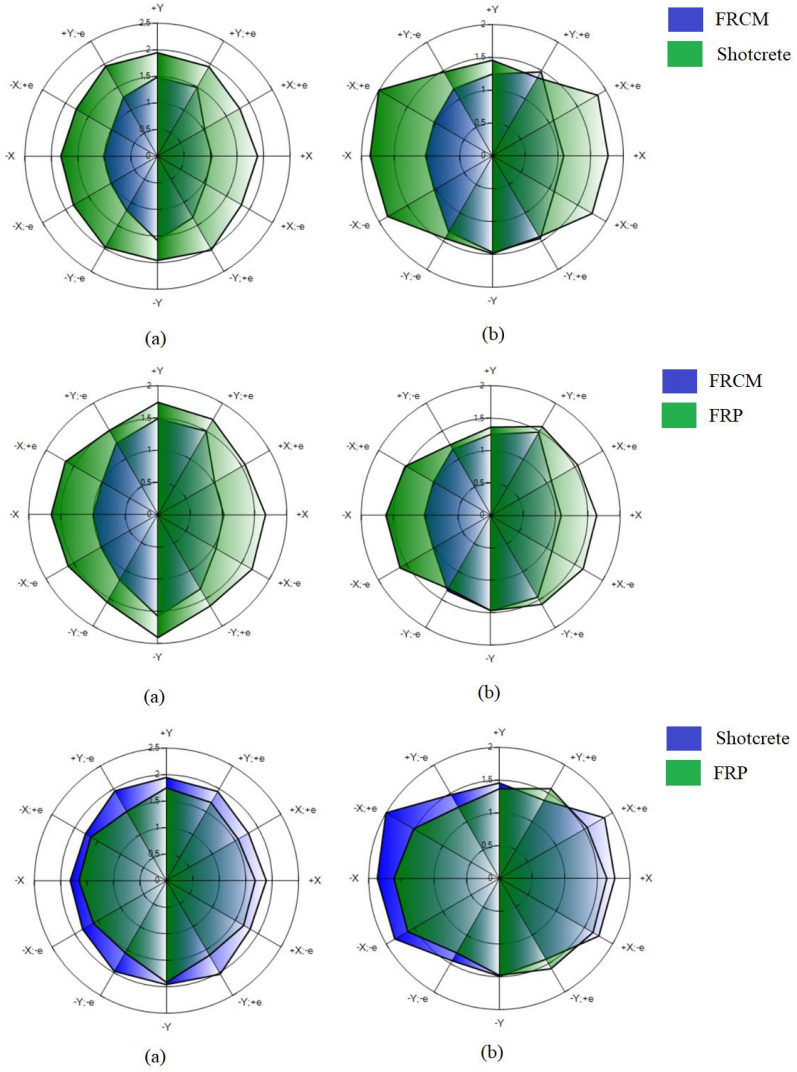

Figure 25. Comparison of vulnerability indices (Significant Damage limit state) of the different strengthening methods: (**a**) uniform load distribution; (**b**) modal load distribution.

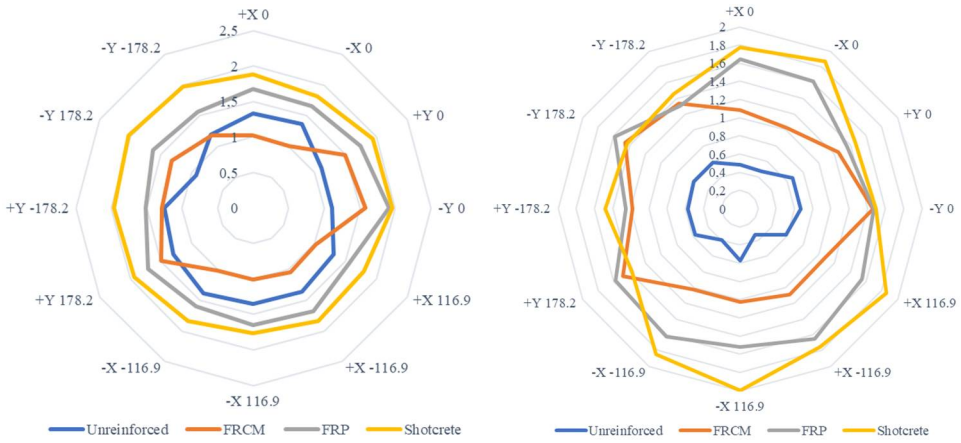

Figure 26. Comparison of vulnerability indices (Significant Damage limit state) of the unreinforced model and all strengthening methods (uniform load distribution—(**left**), modal load distribution—(**right**)).

4. Financial Costs and CO_2 Impact

Besides achieved earthquake capacity, the methods were compared based on cost-effectiveness. Approximate costs of renovation were calculated for every strengthening method (Tables 8–12) according to [75]. The cost of a new concrete slab on the first floor is added to the renovation costs of each strengthening variant, given that the assumption of a rigid diaphragm was a precondition for the limit state checks to be satisfied.

Current trends in the construction industry indicate a general shift toward sustainability and integrated approaches [76,77]; therefore, the environmental impact of the proposed strengthening methods was also considered. In addition, preserving cultural heritage is not only an obligation to sustain and transmit it to the future generation, but is also a driver of sustainable growth [78]. Using the SimaPro software [79], the environmental impact of each strengthening method was calculated in the form of CO_2 greenhouse gas emissions (Table 13). It is important to note that the calculation doesn't take into account CO_2 emissions during transportation, construction, usage, and demolition, but only during the material production phase.

Table 8. Calculation of renovation costs—rigid diaphragm on the first floor.

Task Description	Unit of Measure	Unit price (EUR)	Amount	Total Price (EUR)
Dismantling of existing wooden floor layers	m^2	5.98	491.74	2940.61
Loading and unloading the waste in the landfill	m^3	46.48	24.59	1142.80
Filling the space between the joists with expanded polystyrene (EPS)	m^2	7.3	491.74	3589.70
Installation of steel connectors	pcs	1.59	12,300.00	19,557.00
Installation of anchor rods that connect the concrete slab to the walls	pcs	33.2	360.00	11,952.00
Placement of nylon on which the concrete is poured	m^2	0.66	491.74	324.55
Installation of reinforcement mesh	kg	1.33	2203.00	2929.99
Pouring a new concrete slab (6 cm thick)	m^3	112.88	29.05	3279.16
Total (EUR)			45,715.81	

Table 9. Calculation of renovation costs—preparatory works (all strengthening methods).

Task Description	Unit of Measure	Unit Price (EUR)	Amount	Total Price (EUR)
Operating the mobile scaffolding to perform the necessary task	m^2	15.94	1544.69	24,622.30
Complete removal of plaster from the walls	m^2	4.65	3151.16	14,652.89
Waste collection	m^2	1.99	3151.16	6270.81
Loading and unloading the waste in the landfill	m^3	46.48	94.54	4394.42
Total (EUR)			49,940.30	

Table 10. Calculation of renovation costs—FRCM composite system.

Task Description	Unit of Measure	Unit Price (EUR)	Amount	Total Price (EUR)
Preparatory works				49,940.30
Repointing mortar joints	m^2	13.28	884.36	11,744.32
Application of FRCM system	m^2	33.2	2927.24	97,184.27
Connecting the FRCM layers with FRP rope	pcs	15.94	3500.00	55,790.00
Applying new plaster	m^2	11.28	3151.16	35,545.08
Total (EUR)			250,204.09	

Table 11. Calculation of renovation costs—FRP composite system.

Task Description	Unit of Measure	Unit Price (EUR)	Amount	Total Price (EUR)
Preparatory works				49,940.30
Repointing mortar joints	m^2	13.28	884.36	11,744.32
Application of FRP system	m^2	66.4	2927.24	194,368.54
Connecting the FRP layers with FRP rope	pcs	15.94	3500.00	55,790.00
Applying new plaster	m^2	11.29	3151.16	35,576.60
Total (EUR)		347,419.87		

Table 12. Calculation of renovation costs—shotcrete.

Task Description	Unit of Measure	Unit Price (EUR)	Amount	Total Price (EUR)
Preparatory works				49,940.30
Installation of anchors for the reinforcement mesh (4 pcs/m^2)	pcs	2.66	2710	7208.60
Installation of Q283 reinforcement mesh	kg	1.33	3031.08	4031.34
Shotcrete application (6 cm thick)	m^3	112.88	39.57	4466.46
Applying new plaster	m^2	11.29	3151.16	35,576.60
Total (EUR)		101,223.41		

Table 13. CO_2 emissions for different materials.

	Unit	CO_2 Emissions (kg)	Amount	Total CO_2 Emissions (kg)
FRCM				
Concrete	m^3	385.32	43.91	16,919.25
Glass fiber	kg	1.92	1857.86	3570.00
Total				20,489.25
FRP				
Carbon fiber	kg	31.00	1112.35	34,482.85
Total				34,482.85
Shotcrete				
Concrete	m^3	385.32	40.59	15,640.00
Steel	kg	2.28	3031.08	6900.00
Total				22,540.00

The final goal of this paper is to compare the strengthening methods based on the achieved earthquake capacity, cost, and environmental impact (Figure 27). The diameter of the bubbles represents the CO_2 emissions. The production of concrete emits the largest amount of CO_2 but, from an economic standpoint, this option is the most favorable. Furthermore, glass fibers have a much smaller carbon footprint than concrete and, despite the slightly higher price, the application of the FRCM system should be seriously considered. The FRP system, despite low CO_2 emissions, is quite costly compared to the other variants.

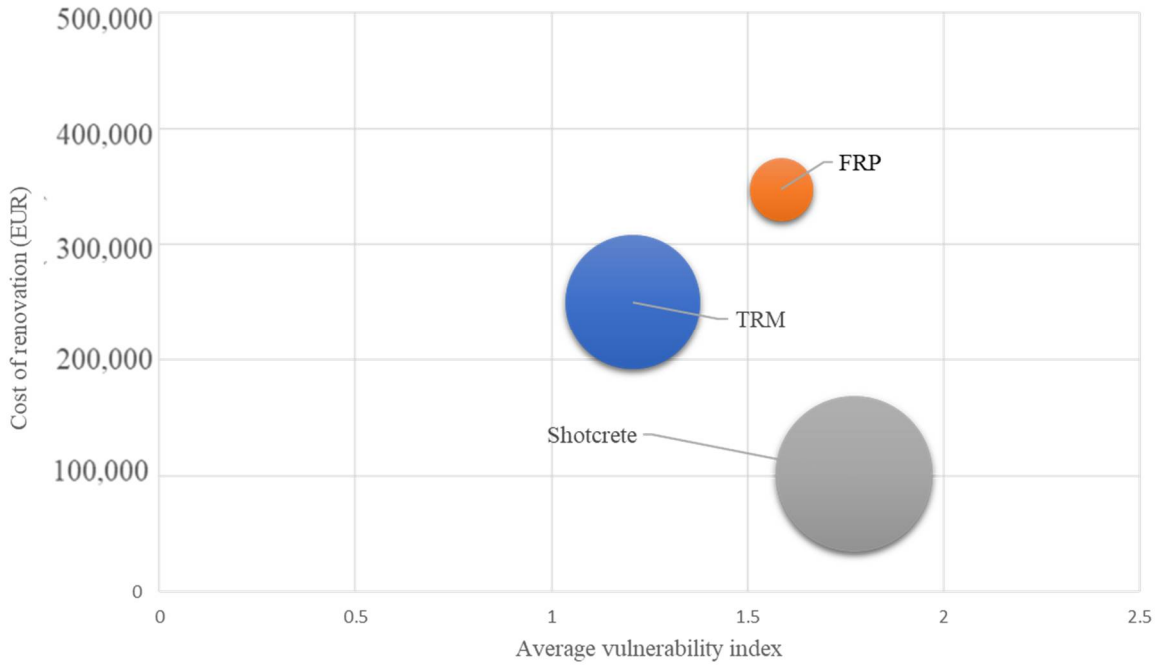

Figure 27. Comparison of methods based on renovation costs, average vulnerability index, and environmental impact.

5. Conclusions

Croatia is one of the most seismically vulnerable countries in Europe. The recent earthquakes in Zagreb and Petrinja exposed many weaknesses of construction in Croatia—dilapidated buildings and materials, numerous mistakes in design and construction, and slow and inconsistent legal framework related to reconstruction are just some of the problems. Experts in the fields of seismology and civil engineering have been warning about the possible catastrophic consequences of earthquakes for years; unfortunately, until the 2020 earthquakes, more attention and resources were directed to increasing the energy efficiency of buildings, while seismic renovation was neglected despite the significant seismic risk.

The main goal of retrofitting is to make buildings earthquake-resistant and to stabilize the current structure. However, in addition, it needs to be in line with the conservation and restoration rules and, of course, with the building owner requests. Some of the basic and commonly used retrofitting methods in Croatia are adding shear walls, jacketing of beams and columns, applying FRCM or FRP, applying shotcrete, and adding timber–concrete composite floors. Shotcreting is certainly more widespread because it is much simpler and certainly ensures a sufficient level of load capacity. The problem arises that it is not effective with flexible diaphragms and greatly changes the static and dynamic image of the lateral system. Renovation with FRP allows the freedom to use the flexible floor structure and, as a rule, does not change the dynamic image of the structure. Basic problems in Croatia are non-educated and untrained workers, high costs of retrofitting, and sometimes unrealistic conservation demands.

The selection of the optimal strengthening method will depend on the age and type of the building, required load-bearing capacity and ductility, available means of reconstruction, and many other factors. Shotcrete is the most cost-effective, but large CO_2 emissions and invasiveness are reasons to consider other solutions, especially when a culturally significant building is in question. The FRP composite system achieved satisfactory seismic capacity; the disadvantage of this solution is the high cost of renovation compared to the FRCM system, which meets the requirements for seismic capacity and sustainability while maintaining a slightly lower price.

Author Contributions: Conceptualization, M.S.; methodology, M.S. and I.M.; software, A.S. and M.K.; validation, A.S. and M.S.; formal analysis, A.S. and M.K.; investigation, A.S. and M.S.; resources, M.S. and I.M.; data curation, A.S.; writing—original draft preparation, A.S. and M.S.; writing—review and editing, A.S. and M.S.; visualization, A.S. and M.S.; supervision, M.S. and I.M; project administration, M.S. and I.M.; funding acquisition, M.S. All authors have read and agreed to the published version of the manuscript.

Funding: This research was funded by the Croatian Science Foundation, grant number UIP-2019-04-3749 (ARES project—Assessment and rehabilitation of existing structures—development of contemporary methods for masonry and timber structures), project leader: Mislav Stepinac.

Data Availability Statement: The data presented in this study are available on request from the corresponding author. The data are not publicly available due to privacy reasons.

Acknowledgments: The authors want to thank Boja Čačić Šipoš for helping in the condition assessment and numerical modeling of the case-study building.

Conflicts of Interest: The authors declare no conflict of interest.

References

1. Bilgin, H.; Shkodrani, N.; Hysenlliu, M.; Baytan Ozmen, H.; Isik, E.; Harirchian, E. Damage and performance evaluation of masonry buildings constructed in 1970s during the 2019 Albania earthquakes. *Eng. Fail. Anal.* **2022**, *131*, 105824. [CrossRef]
2. Papadimitriou, P.; Kapetanidis, V.; Karakonstantis, A.; Spingos, I.; Kassaras, I.; Sakkas, V.; Kouskouna, V.; Karatzetzou, A.; Pavlou, K.; Kaviris, G.; et al. First results on the Mw = 6.9 Samos earthquake of 30 October 2020. *Bull. Geol. Soc. Greece* **2020**, *56*, 251–279. [CrossRef]
3. Vlachakis, G.; Vlachaki, E.; Lourenço, P.B. Learning from failure: Damage and failure of masonry structures, after the 2017 Lesvos earthquake (Greece). *Eng. Fail. Anal.* **2020**, *117*, 104803. [CrossRef]
4. Günaydin, M.; Atmaca, B.; Demir, S.; Altunişik, A.C.; Hüsem, M.; Adanur, S.; Ateş, Ş.; Angin, Z. Seismic damage assessment of masonry buildings in Elazığ and Malatya following the 2020 Elazığ-Sivrice earthquake, Turkey. *Bull. Earthq. Eng.* **2021**, *19*, 2421–2456. [CrossRef]
5. Yakut, A.; Sucuoğlu, H.; Binici, B.; Canbay, E.; Donmez, C.; İlki, A.; Caner, A.; Celik, O.C.; Ay, B.Ö. Performance of structures in İzmir after the Samos island earthquake. *Bull. Earthq. Eng.* **2021**, *20*, 7793–7818. [CrossRef]
6. Stepinac, M.; Lourenço, P.B.; Atalić, J.; Kišiček, T.; Uroš, M.; Baniček, M.; Šavor Novak, M. Damage classification of residential buildings in historical downtown after the ML5.5 earthquake in Zagreb, Croatia in 2020. *Int. J. Disaster Risk Reduct.* **2021**, *56*, 102140. [CrossRef]
7. Moretić, A.; Stepinac, M.; Lourenço, P.B. Seismic upgrading of cultural heritage—A case study using an educational building in Croatia from the historicism style. *Case Stud. Constr. Mater.* **2022**, *17*, e01183. [CrossRef]
8. *World Bank Report: Croatia Earthquake—Rapid Damage And Needs Assessment*; June 2020; Government of Croatia: Zagreb, Croatia, 2020.
9. Comisión Sismológica Europea. *Escala Macro Sísmica Europea EMS—98*; Comisión Sismológica Europea: Luxembourg, 1998; Volume 15, ISBN 2879770084.
10. *World Bank Report: Croatia December 2020 Earthquake—Rapid Damage And Needs Assessment*; Government of Croatia: Zagreb, Croatia, 2021.
11. *The Database of Usability Classification, Croatian Centre of Earthquake Engineering (HCPI—Hrvatski Centar za Potresno Inženjerstvo)*; Faculty of Civil Engineering, University of Zagreb: Zagreb, Croatia, 2020.
12. Atalic, J.; Savor Novak, M.; Uros, M. Rizik od potresa za Hrvatsku: Pregled istraživanja i postojećih procjena sa smjernicama za budućnost. *Građevinar* **2019**, *71*, 923–947.
13. Šipoš, T.K.; Hadzima-Nyarko, M. Seismic risk of Croatian cities based on building's vulnerability. *Teh. Vjesn.* **2018**, *25*, 1088–1094. [CrossRef]
14. Perrone, D.; O'Reilly, G.J.; Monteiro, R.; Filiatrault, A. Assessing seismic risk in typical Italian school buildings: From in-situ survey to loss estimation. *Int. J. Disaster Risk Reduct.* **2020**, *44*, 101448. [CrossRef]
15. O'Reilly, G.J.; Perrone, D.; Fox, M.; Monteiro, R.; Filiatrault, A. Seismic assessment and loss estimation of existing school buildings in Italy. *Eng. Struct.* **2018**, *168*, 142–162. [CrossRef]
16. Gaetani d'Aragona, M.; Polese, M.; Prota, A. Stick-IT: A simplified model for rapid estimation of IDR and PFA for existing low-rise symmetric infilled RC building typologies. *Eng. Struct.* **2020**, *223*, 111182. [CrossRef]
17. Domaneschi, M.; Zamani Noori, A.; Pietropinto, M.V.; Cimellaro, G.P. Seismic vulnerability assessment of existing school buildings. *Comput. Struct.* **2021**, *248*, 106522. [CrossRef]
18. Fontana, C.; Cianci, E.; Moscatelli, M. Assessing seismic resilience of school educational sector. An attempt to establish the initial conditions in Calabria Region, southern Italy. *Int. J. Disaster Risk Reduct.* **2020**, *51*, 101936. [CrossRef]
19. Ruggieri, S.; Chatzidaki, A.; Vamvatsikos, D.; Uva, G. Reduced-order models for the seismic assessment of plan-irregular low-rise frame buildings. *Earthq. Eng. Struct. Dyn.* **2022**, *51*, 3327–3346. [CrossRef]

20. Leggieri, V.; Ruggieri, S.; Zagari, G.; Uva, G. Appraising seismic vulnerability of masonry aggregates through an automated mechanical-typological approach. *Autom. Constr.* **2021**, *132*, 103972. [CrossRef]
21. Longobardi, G.; Formisano, A. Seismic vulnerability assessment and consolidation techniques of ancient masonry buildings: The case study of a Neapolitan Masseria. *Eng. Fail. Anal.* **2022**, *138*, 106306. [CrossRef]
22. Brunelli, A.; de Silva, F.; Cattari, S. Site effects and soil-foundation-structure interaction: Derivation of fragility curves and comparison with Codes-conforming approaches for a masonry school. *Soil Dyn. Earthq. Eng.* **2022**, *154*, 107125. [CrossRef]
23. Law on the Reconstruction of Earthquake-Damaged Buildings in the City of Zagreb, Krapina-Zagorje County and Zagreb County (NN 102/2020). Available online: https://narodne-novine.nn.hr/clanci/sluzbeni/2020_09_102_1915.html (accessed on 29 June 2021).
24. Law on Reconstruction of Earthquake-Damaged Buildings in the City of Zagreb, Krapina-Zagorje County, Zagreb County, Sisak-Moslavina County and Karlovac County (NN 102/2020, 10/21). Available online: https://www.zakon.hr/z/2656/Zakon-o-obnovi-zgrada-o%C5%A1te%C4%87enih-potresom-na-podru%C4%8Dju-Grada-Zagreba%2C-Krapinsko-zagorske-%C5%BEupanije%2C-Zagreba%C4%8Dke-%C5%BEupanije%2C-Sisa%C4%8Dko-moslava%C4%8Dke-%C5%BEupanije-i-Karlova%C4%8Dke-%C5%BEupani (accessed on 29 June 2021).
25. Tehnički Propis o Izmjeni i Dopunama Tehničkog Propisa za Građevinske Konstrukcije. Available online: https://narodne-novine.nn.hr/clanci/sluzbeni/2020_07_75_1448.html (accessed on 29 June 2021).
26. HRN EN 1998-3:2011 Eurocode 8: Design of Structures for Earthquake Resistance—Part 3: Assessment and Retrofitting of Buildings (EN 1998-3:2005+AC:2010). Available online: https://www.phd.eng.br/wp-content/uploads/2014/07/en.1998.3.2005.pdf (accessed on 29 June 2021).
27. Mazzoni, S.; Castori, G.; Galasso, C.; Calvi, P.; Dreyer, R.; Fischer, E.; Fulco, A.; Sorrentino, L.; Wilson, J.; Penna, A.; et al. 2016–2017 central italy earthquake sequence: Seismic retrofit policy and effectiveness. *Earthq. Spectra* **2018**, *34*, 1671–1691. [CrossRef]
28. Calderoni, B.; Cordasco, E.A.; Del Zoppo, M.; Prota, A. Damage assessment of modern masonry buildings after the L'Aquila earthquake. *Bull. Earthq. Eng.* **2020**, *18*, 2275–2301. [CrossRef]
29. Penna, A.; Morandi, P.; Rota, M.; Manzini, C.F.; da Porto, F.; Magenes, G. Performance of masonry buildings during the Emilia 2012 earthquake. *Bull. Earthq. Eng.* **2014**, *12*, 2255–2273. [CrossRef]
30. Bertolini Cestari, C.; Marzi, T. Conservation of historic timber roof structures of Italian architectural heritage: Diagnosis, assessment, and intervention. *Int. J. Archit. Herit.* **2018**, *12*, 632–665. [CrossRef]
31. Thöns, S. Value of Information analyses and decision analyses types. In Proceedings of the COST TU 1402 Training School of Structural Health Monitoring Information, Lake Como, Cadenabbia, Italy, 6–9 November 2017.
32. Scala, S.A.; Del Gaudio, C.; Verderame, G.M. Influence of construction age on seismic vulnerability of masonry buildings damaged after 2009 L'Aquila earthquake. *Soil Dyn. Earthq. Eng.* **2022**, *157*, 107199. [CrossRef]
33. Stepinac, M.; Kisicek, T.; Renić, T.; Hafner, I.; Bedon, C. Methods for the assessment of critical properties in existing masonry structures under seismic loads-the ARES project. *Appl. Sci.* **2020**, *10*, 1576. [CrossRef]
34. Sigmund, Z.; Radujkovic, M.; Lazarevic, D. Decision support model for seismic strengthening technology selection of masonry buildings. *Teh. Vjesn. Technol. Gaz.* **2016**, *23*, 791–800. [CrossRef]
35. Kouris, L.A.S.; Triantafillou, T.C. State-of-the-art on strengthening of masonry structures with textile reinforced mortar (TRM). *Constr. Build. Mater.* **2018**, *188*, 1221–1233. [CrossRef]
36. Kišiček, T.; Stepinac, M.; Renić, T.; Hafner, I.; Lulić, L. Strengthening of masonry walls with FRP or TRM. *Gradjevinar* **2020**, *72*, 937–953. [CrossRef]
37. Ghiassi, B.; Milani, G. *Numerical Modeling of Masonry and Historical Structures: From Theory to Application*; Woodhead Publishing: Sawston, UK, 2019.
38. Bournas, D.A. Concurrent seismic and energy retrofitting of RC and masonry building envelopes using inorganic textile-based composites combined with insulation materials: A new concept. *Compos. Part B Eng.* **2018**, *148*, 166–179. [CrossRef]
39. Al-Lami, K.; D'Antino, T.; Colombi, P. Durability of fabric-reinforced cementitious matrix (FRCM) composites: A review. *Appl. Sci.* **2020**, *10*, 1714. [CrossRef]
40. Rahman, S.; Akib, S.; Khan, M.T.R.; Shirazi, S.M. Experimental study on tsunami risk reduction on coastal building fronted by sea wall. *Sci. World J.* **2014**, *2014*, 729357. [CrossRef]
41. Skejić, D.; Lukačević, I.; Ćurković, I.; Čudina, I. Application of steel in refurbishment of earthquake-prone buildings. *Gradjevinar* **2020**, *72*, 955–966. [CrossRef]
42. Cao, X.Y.; Shen, D.; Feng, D.C.; Wang, C.L.; Qu, Z.; Wu, G. Seismic retrofitting of existing frame buildings through externally attached sub-structures: State of the art review and future perspectives. *J. Build. Eng.* **2022**, *57*, 104904. [CrossRef]
43. Triantafillou, T.C.; Bournas, D.A.; Gkournelos, P. *Novel Technologies for the Seismic Upgrading of Existing European Buildings*; Publications Office of the European Union: Luxembourg, 2022; JRC123314. [CrossRef]
44. Karic, A.; Atalić, J.; Kolbitsch, A. Seismic vulnerability of historic brick masonry buildings in Vienna. *Bull. Earthq. Eng.* **2022**, *20*, 4117–4145. [CrossRef]
45. Blagojević, P.; Brzev, S.; Cvetković, R. Simplified Seismic Assessment of Unreinforced Masonry Residential Buildings in the Balkans: The Case of Serbia. *Buildings* **2021**, *11*, 392. [CrossRef]
46. Available online: http://ss-petrinja.skole.hr/upload/ss-petrinja/newsattach/1020/Dan%20%B9kole-bro%B9ura.pdf (accessed on 2 June 2022).

47. Uroš, M.; Todorić, M.; Crnogorac, M.; Atalić, J.; Šavor Novak, M.; Lakušić, S. (Eds.) *Potresno Inženjerstvo—Obnova Zidanih Zgrada*; Građevinski fakultet, Sveučilišta u Zagrebu: Zagreb, Croatia, 2021; ISBN 978-953-8163-43-7.
48. Pojatina, J.; Barić, D.; Anđić, D.; Bjegović, D. Structural renovation of residential building in Zagreb after the 22 March 2020 earthquake. *Gradjevinar* **2021**, *73*, 633–648. [CrossRef]
49. Lulić, L.; Ožić, K.; Kišiček, T.; Hafner, I.; Stepinac, M. Post-earthquake damage assessment-case study of the educational building after the zagreb earthquake. *Sustainability* **2021**, *13*, 6353. [CrossRef]
50. Stepinac, M.; Rajčić, V.; Barbalić, J. Pregled i ocjena stanja postojećih drvenih konstrukcija. *Gradjevinar* **2017**, *69*, 861–873. [CrossRef]
51. Funari, M.F.; Pulatsu, B.; Szabó, S.; Lourenço, P.B. A solution for the frictional resistance in macro-block limit analysis of non-periodic masonry. *Structures* **2022**, *43*, 847–859. [CrossRef]
52. Santos, F.A.; Caroço, C.; Amendola, A.; Miniaci, M.; Fraternali, F. A concurrent micro/macro fe-model optimized with a limit analysis tool for the assessment of dry-joint masonry structures. *Int. J. Multiscale Comput. Eng.* **2022**, *20*, 53–64. [CrossRef]
53. Tomić, I.; Vanin, F.; Božulić, I.; Beyer, K. Numerical simulation of unreinforced masonry buildings with timber diaphragms. *Buildings* **2021**, *11*, 205. [CrossRef]
54. Asıkoğlu, A.; Vasconcelos, G.; Lourenço, P.B. Overview on the nonlinear static procedures and performance-based approach on modern unreinforced masonry buildings with structural irregularity. *Buildings* **2021**, *11*, 147. [CrossRef]
55. 3muri User Manual 12.2.1. Available online: https://www.3muri.com/en/brochures-and-manuals/ (accessed on 3 July 2022).
56. HRN EN 1996-1-1:2012 Eurocode 6: Design of Masonry Structures—Part 1-1: General Rules for Reinforced and Unreinforced Masonry Structures (EN 1996-1-1:2005+A1:2012). Available online: https://www.phd.eng.br/wp-content/uploads/2015/02/en.1996.1.1.2005.pdf (accessed on 2 June 2022).
57. Lagomarsino, S.; Penna, A.; Galasco, A.; Cattari, S. TREMURI program: An equivalent frame model for the nonlinear seismic analysis of masonry buildings. *Eng. Struct.* **2013**, *56*, 1787–1799. [CrossRef]
58. Penna, A.; Bracchi, S.; Salvatori, C.; Morandini, C.; Rota, M. Extending Analysis Capabilities of Equivalent Frame Models for Masonry Structures. In *European Conference on Earthquake Engineering and Seismology*; Springer: Cham, Switzerland, 2022; pp. 473–485. [CrossRef]
59. Lagomarsino, S.; Cattari, S.; Angiolilli, M.; Bracchi, S.; Rota, M.; Penna, A. Modelling and seismic response analysis of existing URM structures. Part 2: Archetypes of Italian historical buildings. *J. Earthq. Eng.* **2022**. [CrossRef]
60. Penna, A.; Rota, M.; Bracchi, S.; Angiolilli, M.; Cattari, S.; Lagomarsino, S. Modelling and seismic response analysis of existing URM structures. Part 1: Archetypes of Italian modern buildings. *J. Earthq. Eng.* **2022**. [CrossRef]
61. HRN EN 1991-1-1:2012 Eurocode 1: Actions on Structures—Part 1-1: General Actions—Densities, Self-Weight, Imposed Loads for Building (EN 1991-1-1:2002+AC:2009). Available online: https://www.phd.eng.br/wp-content/uploads/2015/12/en.1991.1.1.2002.pdf (accessed on 2 June 2022).
62. Herak, M.; Allegretti, I.; Herak, D.; Kuk, V.; Marić, K.; Markušić, S.; Sović, I. Maps of Seismic Areas of the Republic of Croatia. Available online: https://www.bib.irb.hr/615698 (accessed on 2 June 2022).
63. Krolo, J.; Damjanović, D.; Duvnjak, I.; Smrkić, M.F.; Bartolac, M.; Košćak, J. Methods for determining mechanical properties of walls. *Gradjevinar* **2021**, *73*, 127–140. [CrossRef]
64. Milić, M.; Stepinac, M.; Lulić, L.; Ivanišević, N.; Matorić, I.; Šipoš, B.Č.; Endo, Y. Assessment and Rehabilitation of Culturally Protected Prince Rudolf Infantry Barracks in Zagreb after Major Earthquake. *Buildings* **2021**, *11*, 508. [CrossRef]
65. Nakamura, Y.; Magenes, G.; Griffith, M. Comparison of pushover methods for simple building systems with flexible diaphragms. In Proceedings of the Australian Earthquake Engineering Society 2014 Conference, Lorne, Victoria, 21–23 November 2014.
66. Mirra, M.; Ravenshorst, G.; de Vries, P.; van de Kuilen, J.W. An analytical model describing the in-plane behaviour of timber diaphragms strengthened with plywood panels. *Eng. Struct.* **2021**, *235*, 112128. [CrossRef]
67. Mirra, M.; Ravenshorst, G.; van de Kuilen, J.-W. Comparing in-plane equivalent shear stiffness of timber diaphragms retrofitted with light and reversible wood-based techniques. *Pract. Period. Struct. Des. Constr.* **2021**, *26*, 04021031. [CrossRef]
68. Brignola, A.; Pampanin, S.; Podestà, S. Experimental evaluation of the in-plane stiffness of timber diaphragms. *Earthq. Spectra* **2012**, *28*, 1687–1709. [CrossRef]
69. Peralta, D.F.; Bracci, J.M.; Hueste, M.B.D. Seismic Behavior of Wood Diaphragms in Pre-1950s Unreinforced Masonry Buildings. *J. Struct. Eng.* **2004**, *130*, 2040–2050. [CrossRef]
70. Ciocci, M.P.; Marques, R.F.P.; Lourenço, P.B. Applicability of FEM and Pushover Analysis to Simulate the Shaking-Table Response of a Masonry Building Model with Timber Diaphragms. 2021. Available online: https://scholar.archive.org/work/7w3zeqlhv5g3lbqbwk7rlh6lm4/access/wayback/https://www.scipedia.com/wd/images/d/df/Draft_Content_751443795p1164.pdf (accessed on 15 July 2022).
71. Adhikari, R.K.; D'Ayala, D.F. Applied element modelling and pushover analysis of unreinforced masonry buildings with flexible roof diaphragm. *COMPDYN Proc.* **2019**, *2*, 3836–3851. [CrossRef]
72. Mirra, M.; Ravenshorst, G. A Seismic Retrofitting Design Approach for Activating Dissipative Behavior of Timber Diaphragms in Existing Unreinforced Masonry Buildings. In *Current Perspectives and New Directions in Mechanics, Modelling and Design of Structural Systems*; CRC Press: Boca Raton, FL, USA, 2022; pp. 1901–1907. [CrossRef]
73. Pantò, B.; Boem, I. Masonry elements strengthened with TRM: A review of experimental, design and numerical methods. *Buildings* **2022**, *12*, 1307. [CrossRef]
74. Galić, J.; Vukić, H.; Andrić, D.; Stepinac, L. *Tehnike Popravaka i Pojačanja Zidanih Zgrada*; Arhitektonski Fakultet: Zagreb, Croatia, 2020.

75. Galić, J.; Vukić, H.; Andrić, D.; Stepinac, L. *Priručnik za Protupotresnu Obnovu Postojećih Zidanih Zgrada*; Arhitektonski Fakultet: Zagreb, Croatia, 2020.
76. Milovanovic, B.; Bagaric, M.; Gaši, M.; Stepinac, M. Energy renovation of the multi-residential historic building after the Zagreb earthquake—Case study. *Case Stud. Therm. Eng.* **2022**, *38*, 102300. [CrossRef]
77. Milovanović, B.; Bagarić, M. How to achieve nearly zero-energy buildings standard. *Gradjevinar* **2020**, *72*, 703–720. [CrossRef]
78. Lourenço, P.B.; Barontini, A.; Oliveira, D.V.; Ortega, J. Rethinking Preventive Conservation: Recent Examples. In *Geotechnical Engineering for the Preservation of Monuments and Historic Sites III.*; CRC Press: Boca Raton, FL, USA, 2022; pp. 70–86. [CrossRef]
79. LCA Software for Informed Change-Makers. Available online: https://simapro.com/ (accessed on 23 June 2022).